NASA TR R-

TECHNICAL REPORT

R- 138A

PERIGEE PROPULSION FOR ORBITAL LAUNCH OF NUCLEAR ROCKETS

By Paul G. Johnson and Frank E. Rom

Lewis Research Center
Cleveland, Ohio

NATIONAL AERONAUTICS AND SPACE ADMINISTRATION
WASHINGTON

NA

NATIONAL AERONAUTICS AND SPACE ADMINISTRATION

TECHNICAL REPORT R-

PERIGEE PROPULSION FOR ORBITAL LAUNCH OF NUCLEAR ROCKETS

By Paul G. Johnson and Frank E. Rom

ABSTRACT

A thrust program called perigee propulsion which minimizes gravity loss is analyzed. Thrust is applied intermittently in regions of high velocity (near successive perigees). The increased energy-addition efficiency yields mass ratios approaching those for impulsive velocity change. Corresponding times to reach desired energy are in days but are still small relative to mission times. For specified orbital-launch missions, perigee-propulsion nuclear-rocket systems are shown to equal continuous-thrust performance with reactor powers an order of magnitude less than those of continuous-thrust systems. Application and operational aspects of perigee propulsion are discussed.

(Initial NASA distribution: 42, Propulsion systems, nuclear; 46, Space mechanics; 48, Space vehicles; 53, Vehicle performance)

NATIONAL AERONAUTICS AND SPACE ADMINISTRATION

TECHNICAL REPORT R-

PERIGEE PROPULSION FOR ORBITAL LAUNCH OF NUCLEAR ROCKETS

By Paul G. Johnson and Frank E. Rom

SUMMARY

The use of a thrust program to maximize energy-addition efficiency during orbital launch of nuclear rockets affects the selection of an initial acceleration. With continuous thrust, the gravity-loss effect typically results in the choice of thrust-to-weight ratios near 0.5. An alternative thrust program is analyzed which can make use of accelerations of less than 0.1 g. Perigee propulsion, which is a means of minimizing the gravity loss, is characterized by intermittent application of thrust in regions of high velocity. The resulting flight path would consist of a series of powered segments occurring near successive perigees separated by elliptic coasting segments. The increased energy-addition efficiency yields mass ratios approaching those for impulsive velocity change. Although corresponding times to reach desired energy are measured in days rather than minutes, they are still small relative to mission times measured in months.

The perigee propulsion trajectory analysis evaluates the possible compromises between mass ratio and time to reach desired energy, and a comparison of perigee-propulsion and continuous-thrust systems is made in terms of residual loads for specified missions. The primary advantage of perigee propulsion over continuous thrust is a reduction in required reactor power. A specified vehicle weight can be propelled by a powerplant of lower thrust, or a given powerplant can be used in a larger spacecraft when perigee propulsion is utilized. For example, the optimum power for a 50,000-pound vehicle using continuous thrust is equal to the optimum power for a 500,000-pound spacecraft using perigee propulsion. No significant penalties due to afterheat-removal or control requirements are apparent. Radiation-belt exposure times are intermediate between those of high-acceleration chemical or nuclear-powered vehicles and electric-propulsion spacecraft.

INTRODUCTION

For interplanetary flight from an orbit about Earth, the selection of initial acceleration is a compromise among many factors. For nuclear rockets the factors most commonly considered are (1) the variation of

powerplant weight with power, (2) the variation of specific impulse with hydrogen pressure, and (3) gravity loss. The latter is the overwhelming influence which dictates that the initial thrust-to-weight ratio be relatively high (typically near 0.5) for continuous-thrust trajectories. However, thrust need not be continuous; the thrust schedule is another factor which can be varied in the optimization of initial acceleration. Since low-acceleration continuous-thrust propulsion results in a long spiral trajectory, much of the energy is added at low velocity. The resulting energy-addition efficiency is less than that for impulsive acceleration. Use of some form of thrust program to improve the efficiency of energy addition appears to be the only way of economically applying low-thrust nuclear powerplants (producing initial accelerations less than 0.1 g) to interplanetary propulsion.

A thrust program which minimizes gravity loss and is compatible with nuclear-rocket propulsion is described herein, under the name perigee propulsion. In this scheme, thrust is intermittent, being applied only in the regions of highest velocity, which are near the successive perigees. Energy addition at high velocity results in an appreciable gain in efficiency. Between thrust periods, the spacecraft coasts in an elliptic path about Earth until the desired position relative to the next perigee is reached and thrust is resumed. When escape energy or some lower specified value is attained, thrust becomes continuous until the desired final energy is reached.

The improvement in efficiency resulting from the use of perigee propulsion is gained at the expense of increased overall propulsion time, that is, time to reach final energy. However, since most continuous-thrust propulsion times are of the order of minutes or hours, an increase of several orders of magnitude can be accepted before perigee-propulsion times become significant relative to total mission times, which are usually measured in months.

A similar "pulsed flight plan" for electrical propulsion systems is illustrated in reference 1, where electrical-energy storage is included as an additional advantageous feature. The applications cited, transfer between terrestrial circular orbits of different radii and satellite rendezvous, emphasize the effect of energy storage, but the scheduling of powered and unpowered flight is very similar to that of perigee propulsion. Reference 2 examines the limiting case of extremely small, impulsive bursts at perigee and concludes that the time penalties corresponding to "very low thrust" would be prohibitive. An example supporting this conclusion corresponds roughly to perigee propulsion with initial acceleration of 10^{-4} g. A more favorable example, called an "artificial case" because the bursts are too large to fit the author's "very low thrust" criterion, closely approximates the performance of a nuclear rocket using perigee propulsion with an initial acceleration of 0.01 g.

The purposes of the present study are to present quantitative results and to assess the overall effects of the mass-ratio - time compromise. The results are presented in the form of charts which can be used to determine the approximate characteristics of any perigee propulsion trajectory within the parameter ranges covered. The analysis is based on numerical integrations of powered-flight trajectories with assumed values of specific impulse, initial acceleration, angle subtended by each powered-flight segment, and angular position at which thrust is initiated for each power-on cycle. These parameters are held constant for each flight but are assigned several values when optimum conditions are being determined. Finally, a preliminary evaluation of the worth of perigee propulsion is made. Consideration is given to the increased demands upon the propulsion system in terms of such items as control, afterheat removal, and temperature cycling. Operational problems such as vehicle control and space-radiation shielding are discussed qualitatively.

METHODS AND ASSUMPTIONS

General Procedure

The mass ratio W_G/W_E and total time t_t required to attain an energy level equivalent to a specified hyperbolic velocity v_h are computed for various values of (1) specific impulse I, (2) initial thrust-to-weight ratio F/W_G, (3) thrust-initiation angular position relative to perigee $\Delta\theta_1$, and (4) thrust-termination angular position $\Delta\theta_2$. (Symbols are defined in appendix.) The latter two parameters, which define the length and orientation of the powered-flight segments, are subject to optimization in terms of minimum mass ratio at a given total time to achieve the desired hyperbolic velocity. Optimization of thrust-to-weight ratio would have to be made in terms of payload for a specified mission and would require knowledge of component-weight and performance variations with thrust level as well as the characteristics of the interplanetary trajectories involved. The results of the analysis include optimization of $\Delta\theta_1$ and $\Delta\theta_2$ and the effects of variations in I, F/W_G, and v_h, so that optimization of F/W_G can be accomplished for any desired combination of powerplant, vehicle, and mission characteristics.

A schematic representation of a perigee-propulsion escape trajectory is shown in figure 1. The illustration is idealized to the extent that the successive perigees are shown superimposed, whereas, in reality, the perigee altitude increases slightly and the perigee position shifts in a counterclockwise direction as the flight progresses. However, the essential nature of the composite path is shown, with each propulsion period followed by an elliptic coasting path to a point $\Delta\theta_1$ degrees before

the next perigee. During the final propulsion period escape energy or a specified lower value is reached, and the thrust is made continuous from that point until final energy is attained.

Since the last elliptic coast periods consume a major portion of the total time, variations on the basic flight plan are analyzed wherein continuous-thrust is begun in propulsion periods prior to the one in which escape energy is attained. Elimination of the last coast period, for example, may cut the total time by a factor of 3 while increasing the mass ratio by only 1 percent. Regression to earlier perigees has a diminishing effect on total time while causing progressive deterioration of mass ratio. The compromise which should be chosen depends upon particular mission requirements.

Basic Assumptions

The analysis is based on the assumption that the Earth can be represented by an inverse-square central force field. Thus all perturbing effects, such as oblateness and lunar gravity, are neglected in the computations. The radius of the Earth is taken to be 3958.9 miles, and its force constant μ is assumed to be 95,636.5 miles^3/sec^2.

During the powered-flight segments, specific impulse and thrust are assumed to remain constant, and the thrust is maintained at a fixed angle β to the vehicle velocity. The thrust orientation is optimized in a preliminary manner. The times required to raise and lower reactor power at the beginning and end of each propulsion period are assumed to be negligible in relation to powered flight time. Likewise, any thrust due to the flow of afterheat-removal coolant during the coast periods is neglected. The amount of propellant required for afterheat removal is not included in the results presented, but an indication of this small effect is included in the discussion of results.

Powered-Flight Analysis

Computation of the trajectories during periods of thrust application is accomplished by numerical integration of the equations of motion on a digital computer. The particular forms of the equations used in the analysis are as presented in reference 3. A Runge-Kutta numerical-integration procedure is used to obtain solutions.

The nomenclature and conventions used in the powered-flight analysis are shown in figure 2. At any given time the flight conditions are characterized by values of radius r, velocity magnitude v, velocity direction α relative to the local horizontal, and central angle θ relative to either the beginning of the current powered-flight path or the initial-

thrust-initiation point. The thrust has an angle β relative to the velocity vector. The beginning and end of a propulsion period are located relative to the perigee of the previous coasting path by specification of $\Delta\theta_1$ and $\Delta\theta_2$, both considered positive when measured counterclockwise from perigee. ($\Delta\theta_1$ is negative in fig. 2.)

Coasting Flight Analysis

After each propulsion period the spacecraft follows an elliptic path to the point designated as the beginning of the next propulsion period. The analysis consists of determinations of (1) the elliptic-orbit elements and (2) the conditions at the start of the next propulsion period from the values of r, v, and α at thrust cutoff. The basic equations relating conditions at the end of the n^{th} propulsion period (subscript $n,2$) to conditions at the perigee of the subsequent coasting ellipse (subscript $n+1,0$) are derived from the equations in reference 4; they are the following:

$$E_n = \frac{v_{n,2}^2}{2} - \frac{\mu}{r_{n,2}} = \frac{v_{n+1,0}^2}{2} - \frac{\mu}{r_{n+1,0}} \tag{1}$$

$$r_{n,2} v_{n,2} \cos \alpha_{n,2} = r_{n+1,0} v_{n+1,0} \tag{2}$$

$$\cos\left[\theta_{n,2} - \theta_{n+1,0} + 2\pi\right] = \frac{\frac{v_{n+1,0}^2 r_{n+1,0}}{\mu} - \frac{r_{n,2}}{r_{n+1,0}}}{\frac{r_{n,2}}{r_{n+1,0}}\left[\frac{v_{n+1,0}^2 r_{n+1,0}}{\mu} - 1\right]} \tag{3}$$

Equations (1) and (2) suffice for determination of perigee radius and velocity. Equation (3) determines the central angle through which the radius vector would turn in going from cutoff to the next perigee.

The same three equations can be used to establish conditions at the beginning of the next propulsion period (subscript $n+1,1$), if $\Delta\theta_1 \equiv \theta_{n+1,1} - \theta_{n+1,0}$ is specified. In the determination of α the angle is said to be positive when the velocity is pointed above the local horizontal.

Similarly, the equation which expresses the time to travel from perigee to any given point on the ellipse can be used to calculate the time between the cutoff of one propulsion period and the beginning of

the next. In terms of conditions at cutoff and perigee, the time equation may be written

$$\Delta t_2 = \frac{\mu}{\left(-v_{h,n}^2\right)^{1.5}} \left(\sin^{-1} \frac{-v_{h,n}^2 \frac{r_{n,2}}{\mu} - 1}{\frac{v_{n+1,0}^2 r_{n+1,0}}{\mu} - 1} + \frac{\pi}{2} - \frac{v_{n+1,0} r_{n+1,0}}{\mu} \sqrt{-v_{h,n}^2} \left| \tan \alpha_{n,2} \right| \right) \tag{4}$$

where Δt_2 is the time of elliptic coasting from perigee to cutoff along the shortest segment of the ellipse (central angle less than 180°) and v_h is the velocity at infinity (hyperbolic velocity) defined by

$$E_n = \frac{v_{h,n}^2}{2} = \frac{v_{n,2}^2}{2} - \frac{\mu}{r_{n,2}} \tag{5}$$

The time of travel between cutoff and the next perigee is found by subtracting Δt_2 from the period of the ellipse:

$$t_{n+1,0} - t_{n,2} = \frac{\mu}{\left(-v_{h,n}^2\right)^{1.5}} (2\pi) - \Delta t_2 \tag{6}$$

The time at the beginning of the next propulsion period is obtained by replacing $n,2$ conditions with $n+1,1$ conditions in equation (4) and calculating $\Delta t_1 = t_{n+1,1} - t_{n+1,0}$. Then, the time between successive propulsion periods is given by

$$t_{n+1,1} - t_{n,2} = \frac{\mu}{\left(-v_{h,n}^2\right)^{1.5}} (2\pi) - \Delta t_2 + \Delta t_1 \tag{7}$$

In the calculation of Δt_1 the time increment is given the same sign as $\Delta\theta_1$; that is, if $\Delta\theta_1$ is negative, Δt_1 will be negative, which is opposite in sign from the value calculated from the equivalent of equation (4).

RESULTS OF TRAJECTORY ANALYSIS

Path Characteristics

By use of the computational procedure of the preceding section, the characteristics of the succession of powered and unpowered flight segments can be determined for any combination of I, F/W_G, v_h, $\Delta\theta_1$, $\Delta\theta_2$, β, and $r_{1,0}$. The latter parameter, the initial orbit radius, has been fixed at 4258.9 miles, which is an altitude of 300 statute miles. Also, an optimization of β has resulted in a selection of $\beta = 0$ for the bulk of the computations. Graphical optimization of $\Delta\theta_1$ and $\Delta\theta_2$ has been carried out for most combinations of the following parameter values:

I, lb/(lb/sec)	800, 900, 1000
F/W_G	0.01, 0.03, 0.05
v_h, miles/sec	1.855, 3.0, 5.0

The result of one such calculation is shown in figure 3. The ratio of initial (gross) weight to empty weight at desired energy attainment is plotted as a function of total time, defined as the sum of powered and unpowered periods prior to final thrust termination. The example corresponds to $I = 800$ pounds per pound per second, $F/W_G = 0.03$, $v_h = 3.0$ miles per second, $\Delta\theta_1 = -45^\circ$, and $\Delta\theta_2 = 30^\circ$. The result of such a computation is a series of discrete points such as plotted in figure 3. Each point is the result of starting the final, continuous-thrust propulsion period during a particular powered-flight segment of the perigee-propulsion sequence. The point corresponding to the highest time is the result of using the thrust-programing technique until escape energy is attained and then applying continuous thrust until the desired excess energy is reached. The points at lower times reveal the mass ratios required to reach the same final energy with continuous thrust begun in propulsion periods earlier than that in which escape energy is attained.

Although each computed point is discrete, a curve has been drawn through the points in figure 3. Such action is justifiable because minute changes in $\Delta\theta_1$ and $\Delta\theta_2$ produce large changes in time with negligible changes in mass ratio. Thus, with very small ranges of $\Delta\theta$ a continuous time spectrum is covered. In fact, the resulting graphical representation would be a band of such slight width that it could be represented by a single curve. All subsequently mentioned results are shown as curves, and the optimization process serves to further eliminate any impropriety in the simplification.

An indication of the flight-path characteristics is shown in the following tabulation of conditions at the beginning and end of successive propulsion periods for the same specified conditions as used in figure 3:

Propulsion period	$t_{n,1}$, days	$h_{n,1}$, miles	$v_{n,1}$, miles/sec	$\theta_{n,1}$, deg (a)	$\alpha_{n,1}$, deg	$h_{n,2}$, miles	$v_{n,2}$, miles/sec	$\alpha_{n,2}$, deg
1	0	300	4.74	0	0	400	4.85	2.89
2	.074	430	4.82	82	-3.35	468	5.01	5.05
3	.164	556	4.92	168	-6.52	533	5.18	7.05
4	.275	677	5.05	-105	-9.52	594	5.36	8.88
5	.418	794	5.19	-18	-12.32	651	5.56	10.57
6	.620	905	5.36	70	-14.93	704	5.77	12.10
7	.940	1010	5.54	160	-17.36	754	5.99	13.53
8	1.610	1110	5.74	-113	-19.57	800	6.22	14.83
9	5.280	1205	5.96	23	-21.60	8273	4.96	56.40

[a]In this instance, $\theta_{n,1}$ is measured relative to the position of initial thrust application $\theta_{1,0}$ and is reduced to a magnitude less than 180°. Also, by definition, $\theta_{n,2} = \theta_{n,1} - \Delta\theta_1 + \Delta\theta_2$.

The extent to which the propulsion periods are confined to low altitudes and correspondingly high velocities gives a clear explanation of the performance gains illustrated in figure 3. Although not shown, the perigee altitudes of the elliptic coasting paths of the example remain below 500 miles, which indicates that little could be gained from further efforts to control perigee altitude. By comparison, the final altitude of a continuous-thrust trajectory with the same initial thrust-weight ratio would be 19,720 miles.

Optimization of $\Delta\theta_1$ and $\Delta\theta_2$

The relative position and extent of the several propulsion periods are subject to optimization, and the graphical procedure is illustrated in figures 4 and 5. Specific impulse, initial thrust-weight ratio, and hyperbolic velocity are held constant at the values used in the previous example. The further assumption is made that $\Delta\theta_1$ and $\Delta\theta_2$ are constant throughout a specific flight. Holding $\Delta\theta_1$ constant and computing perigee-propulsion trajectories for several values of $\Delta\theta_2$ result in a set of curves such as shown in figure 4. The envelope of the family, the dotted curve, is the locus of optimum values of $\Delta\theta_2$. Gathering the envelope curves corresponding to several values of $\Delta\theta_1$ results in families like that shown in figure 5. Again, an envelope curve can be drawn which is the locus of optimum $\Delta\theta_1$ and $\Delta\theta_2$ points.

Effects of Parameter Variations

The curves of W_G/W_E against total time for various combinations of I, F/W_G, and v_h which result from the $\Delta\theta$ optimization can be used to illustrate the effects of variations in these parameters. For example, figure 6 is a series of cross plots showing the effect of changing specific impulse from 800 to 1000 pounds per pound per second. The several sections are for all combinations of F/W_G and v_h values considered in the analysis. The downward trend in mass ratio with an increase in I is an obvious expectation. Curves of this type for various combinations of F/W_G and v_h are of quantitative importance because specific impulse undergoes small changes corresponding to variations in optimum hydrogen pressure, and interpolation becomes necessary.

The effect of a change in initial thrust-weight ratio is presented in figure 7. The envelope curves from the $\Delta\theta$ optimization are shown for $F/W_G = 0.01$, 0.03, and 0.05, $I = 800$ pounds per pound per second and $v_h = 3.0$ miles per second. At very large times, the curves approach the impulsive-thrust mass ratio, $\exp(\Delta v/g_c I)$, indicated by the short-dashed line. For an initial thrust-weight ratio of 0.01, the mass ratio appears to reach the region of diminishing returns at times of about 5 to 10 days. For $F/W_G = 0.03$, the corresponding propulsion-time region seems to be 2 to 3 days. The mass ratios continue to decrease as time is increased above these values, however, and the performance comparisons described in the following section indicate that optimum total times may be as high as 20 and 10 days for F/W_G's of 0.01 and 0.03, respectively. In the trajectories corresponding to these total times, the powered-flight segments typically cover a central angle of 60° to 120°.

The effect of a variation in hyperbolic velocity is shown in figure 8, where mass ratio is plotted against v_h for various values of total time. The several sections are for the various combinations of specific impulse and initial thrust-weight ratio. The broken lines show the corresponding impulse mass ratios. Perigee propulsion is indicated to approach impulse performance at lower hyperbolic velocities without excessive total times, but higher v_h's require relatively greater values of either mass ratio or time. Figures 6 and 8 must generally be used together to make the double interpolation between specified values of I and v_h. For continuous thrust the value of v_h would be arbitrarily selected along with the mission and would remain constant as long as the mission was fixed. However, for perigee-propulsion calculations, v_h will vary, since total mission time should be fixed. In the process of optimizing time to reach desired energy, each change in t_t results in a change in coast time. The corresponding change in hyperbolic velocity requires the use of figure 8.

The other parameter variation considered is that of the thrust angle β. Although optimization of β is possible for any combination of other conditions, the present study has not been carried to this extent. Consequently, after spot checks of the effect of variations in β, illustrated in figure 9, a value of $\beta = 0$ was selected for all further calculations. The perigee-propulsion curves in figure 9 show the effect of letting the thrust deviate from the velocity direction by $\pm 5^{\circ}$. The thrust angle was held constant throughout a particular flight, including the final, continuous-thrust maneuver, although there is no indication that constant β would be optimum. The results of several such investigations, typified by figure 9, indicate that $\beta = 0$ is approximately optimum.

PERFORMANCE COMPARISONS

Procedure

A preliminary indication of the worth of the perigee-propulsion thrust-programing technique can be obtained by combining the results of the trajectory analysis with representative vehicle-component weight estimates. Values of residual load, defined as the sum of all fixed weights and the payload, may be computed for vehicles which accomplish a specified mission using the alternative propulsion schedules. A comparison of residual loads provides an initial estimate of the potential gains involved.

The procedure adopted for the initial comparison utilizes a mission in which the vehicle starts from a 300-statute-mile circular Earth orbit and finally attains an energy level that would enable it to reach Mars's vicinity 209 days from the initiation of thrust. The particular trip time chosen corresponds to minimum hyperbolic velocity for one-way Mars probe trajectories in 1960, as shown in the three-dimensional analysis of reference 5. The comparison would not be significantly altered by use of trajectory data for later synodic periods, since only the rate of change of v_h with coast time is important. For low-thrust powerplants, the time required to attain the desired hyperbolic velocity must be included in the 209 days, and the interplanetary coast time is correspondingly shorter. The variation of hyperbolic velocity with coast time, plotted from reference 5 and similar unpublished NASA data, is shown in figure 10.

With the family of paths specified and the powered-flight trajectory characteristics known, the comparison next requires the estimation of mass ratios and powerplant weights. Mass ratios depend upon specific impulse and initial thrust-weight ratio as well as hyperbolic velocity. When a fixed value of reactor-exit hydrogen temperature and equilibrium expansion in a fixed area-ratio nozzle are assumed, the specific impulse

is only a function of reactor-exit pressure, as shown in figure 11. The values of vacuum specific impulse for various temperatures and pressures are from data in reference 6. Thrust, in turn, is a function of specific impulse and flow rate, with the latter being determined by hydrogen temperature and pressure, reactor-exit Mach number, and reactor flow area. For the comparison a gas temperature of 4500° F and a nozzle area ratio of 50 were selected. A fixed Mach number of 0.4 is assumed, although this is not known to be the best form of reactor flow limit. The remaining choice of pressure and flow area is an opportunity for optimization, as shown in reference 7. Such an optimization has been attempted in the comparison computations but only to the extent that the true optimums are approached and the large gains realized.

Mass ratios for constant-thrust vehicles are obtained from charts such as those presented in reference 3, while powerplant weights are those estimated in reference 7. The powerplant weight is composed of the individual weights of the reactor, pressure chamber, nozzle, and turbopump. These weights vary with reactor flow area and hydrogen pressure. Other weights taken into account are (1) tank weight, which is assumed to be 8 percent of propellant weight (ref. 8), and (2) vehicle structure weight, which is assumed to be 2 percent of vehicle initial weight (ref. 7). All such estimates are necessarily preliminary approximations but are believed to serve the purpose. Representative magnitudes are contained in table I, which is described in the section Results of Comparison.

Residual load, used as the comparison parameter, is the difference between empty weight and the sum of powerplant, tank, and structure weights:

$$W_{RL} = W_G\left(\frac{1}{W_G/W_E}\right) - W_{PP} - W_T - W_{ST} \tag{8}$$

Values of residual load have been computed for continuous-thrust vehicles of 500,000 and 50,000 pounds gross weight over a range of initial thrust-weight ratios of 0.01 to 0.5, taking into account the gravity-loss effect, the variation of specific impulse with pressure level, the variation of powerplant weight with flow area and pressure, and the other factors mentioned previously. Corresponding residual loads for perigee-propulsion vehicles have been calculated at F/W_G's of 0.01, 0.03, and 0.05 using the mass-ratio data described herein. At each initial thrust-weight ratio, t_t is approximately optimized, considering the variations of mass ratio and hyperbolic velocity which result from changes in time.

Values of reactor power corresponding to the specified reactor operating conditions have been computed for an assumed propellant inlet

temperature of 200° R, the specific-impulse values of figure 11, and a wide range of reactor-exit temperatures and pressures. The results are shown in figure 12 plotted as the ratio of power to thrust, which is computed from the following equation:

$$\frac{Q}{F} = \frac{H_e - H_i}{I_{vac}} \tag{9}$$

Enthalpy values are taken from reference 6.

Results of Comparison

The performance comparison of perigee propulsion and continuous thrust is presented in figure 13 and table I. Figure 13 shows (1) the variation of residual load, plotted as W_{RL}/W_G, with initial thrust-weight ratio for continuous-thrust nuclear rockets and (2) the corresponding values for perigee propulsion with F/W_G between 0.01 and 0.05. The mission is a 209-day flight from a 300-statute-mile Earth orbit to the vicinity of Mars. Figure 13(a) presents the comparison at an initial vehicle weight of 500,000 pounds, and figure 13(b) presents the corresponding comparison at 50,000 pounds. The approximate conversion from F/W_G to reactor power Q is indicated along the abscissa. The effect of a variation in attainable hydrogen recombination in the nozzle is also shown by use of the two extremes of equilibrium expansion and no dissociation. The latter terminology is used to describe use of a constant specific impulse, evaluated at the specified temperature and a pressure of 1000 pounds per square inch absolute (see fig. 11). The constant I assumption is more of a penalty than frozen flow would be and is used herein only for simplification.

A breakdown of vehicle component weights and other parameters for most of the computed points from which figure 13 was drawn is shown in table I. The two gross weights and representative F/W_G's are included. Values of specific impulse, reactor size, hydrogen pressure, reactor power, power density, and residual load are tabulated. Each calculation involves a rough optimization of pressure, and the perigee-propulsion examples use approximately optimum times to reach desired energy. With equilibrium expansion, optimum pressures are relatively low to take advantage of the increased specific impulse. Reactor flow area remains nearly constant except at the highest accelerations, where the optimum value is reduced somewhat. With constant specific impulse, the optimization of pressure is simply a matter of powerplant weight variation. Higher pressures and smaller reactors are the result for the cases labeled no dissociation. Note that the thrust-programing technique has no effect on the pressure and reactor-size optimization.

Optimum total times for perigee-propulsion applications are shown to be about 20, 10, and 8 days for F/W_G's of 0.01, 0.03, and 0.05, respectively. These times are quite far from the knees in the curves, as can be seen in figure 7. The choice of mission has a large influence on the time optimization. The mission used in the illustrative example involves a relatively slow variation of hyperbolic velocity with Earth-Mars coast time because the basic path is a minimum-energy trajectory. Had a shorter trip time been selected, the optimization would have tended toward shorter t_t's with a consequent small deterioration of perigee-propulsion performance.

The powerplants for the 500,000-pound vehicles are indicated to optimize at higher pressures than those for 50,000-pound vehicles. The values in table I confirm the conclusion in reference 7 that optimum pressure for pump-fed systems is approximately proportional to the square root of the gross weight.

The principal result of the comparison is shown clearly in both parts of figure 13: The use of perigee propulsion permits attainment of performance equal to that of the best continuous-thrust systems but with reactor powers reduced by factors of about 10 to 20. Another way to express the result is that a given powerplant could be used to propel a vehicle of 10 to 20 times the gross weight when perigee propulsion is used instead of continuous thrust. Factors greater than 20 may be observed where perigee-propulsion points exceed maximum continuous-thrust performance. However, the 10 to 20 range expresses the approximate separation of the curves in figure 13.

At thrust-weight ratios greater than 0.05, perigee propulsion may be expected to give residual loads about equal to those for 0.05 but gradually approaching the continuous-thrust values as F/W_G increases. At a thrust-weight ratio near 0.5 the two thrust programs would be identical because the energy addition would be high for either thrust program.

DISCUSSION

Validity of Comparison

The result of the comparison which shows that perigee-propulsion systems with relatively low reactor powers can match continuous-thrust performance cannot be immediately accepted as valid for all conditions. Questions must be answered regarding the effects of (1) changes in mission requirements, (2) changes in powerplant weight assumptions, and (3) operational characteristics peculiar to perigee propulsion. In the latter category, the afterheat-coolant weight requirement appeared to be the greatest threat to the performance margin, and a brief analysis is included to show that its effect is almost negligible.

Effect of mission requirements. - Considering first the effect of mission requirements, two aspects tend to modify the conclusion that perigee-propulsion reactor-power reductions are factors of 10 to 20. The first is the effect of shorter trip times. The 209-day Earth-Mars mission is an actual-orbit minimum-energy path in the particular synodic period selected. Thus, as shown in figure 10, the required hyperbolic velocity changes little with variations in trip time near the minimum-energy condition. Had a faster trip been chosen as the basis for the comparison, the perigee-propulsion systems would have suffered a more severe penalty when coast time was traded for time to reach desired energy. The optimum operating point on the applicable curve of mass ratio against total time (similar to fig. 7) would move to lower values of time.

An indication of the effect on the performance comparison may be obtained from a spot check for a total mission time of 150 days. The results are given in the following table for W_G = 500,000 pounds and no dissociation (I = 860 lb/(lb/sec)):

	Mission time, days							
	150				[a]209			
	Thrust program							
	Perigee propulsion		Continuous thrust		Perigee propulsion		Continuous thrust	
F/W_G	0.03	0.05	0.1	0.5	0.03	0.05	0.1	0.5
W_{RL}/W_G	.507	.522	.467	.523	.546	.564	.505	.555

[a]Data from fig. 13(a).

The conclusion regarding power reduction which can be drawn for the 150-day mission is that perigee-propulsion performance equals that of continuous-thrust systems with reactor powers lower by factors of at least 7 to 10. This result comes from making a plot like figure 13 using the points in the preceding table and comparing powers at equal residual loads. The general result should then be modified to state that the power reduction permitted by perigee propulsion is approximately one order of magnitude.

The second aspect of mission choice which is significant in the comparison of thrust-programing techniques involves the energy required to enter a Martian satellite orbit. The sample calculations take into account only the differences in hyperbolic velocity at Earth, but variations in coast time would also cause differences in hyperbolic velocity

at Mars. If the mission calls for orbiting Mars, the comparison should be based on residual load in Martian orbit. If the hyperbolic velocity at Mars varied with trip time in the same manner as does Earth-departure hyperbolic velocity, the comparison of thrust programs would be the same as for Earth escape only. Unfortunately, the hyperbolic velocity at Mars for minimum-energy paths varies more sharply with trip time than does the hyperbolic velocity at Earth. Thus, the comparison of thrust schedules at Mars for all trip times would be more like that at Earth for the shorter trips, of which 150 days is an example. The overall comparison for orbiting paths would probably be basically similar to that for Earth departure only, but with minimum-energy paths showing slightly less advantage for perigee propulsion than indicated in the 209-day nonorbiting example.

Effect of powerplant weight assumptions. - Considering next the effect of powerplant weight assumptions, a simple calculation can be used to show that the effect is small. For the perigee propulsion calculations tabulated in table I(b), the worst conceivable change in the variation of W_{PP} with A_f would be to assume constant powerplant weight. The largest tabulated difference in powerplant weights (for equilibrium expansion) is about 300 pounds. This amount, when subtracted from the residual load of the low W_{PP} case, results in less than a 2-percent change in W_{RL}/W_G. Performing the same type of transformation with the values in table I(a) results in an even smaller change in W_{RL}/W_G. The effect of raising all powerplant weights by a specified amount or factor would have practically no effect on the relative comparison of thrust programs.

Effects of operational characteristics. - An estimate of the amount of propellant required to remove the reactor afterheat during the coast periods which follow reactor operation is obtained from a simplified calculation. The analysis has two objectives: (1) to estimate afterheat-coolant weight and (2) to determine whether or not this weight is greater for perigee propulsion than for continuous thrust. The afterheat power is obtained by integration of an equation from reference 9 which expresses the rate of beta and gamma energy as a function of time:

$$\frac{Q_{AH}}{Q} = 0.0059\left[(t - t_Q)^{-0.2} - t^{-0.2}\right] \tag{10}$$

where Q_{AH}/Q is the ratio of afterheat to propulsion-period reactor power at time t after reactor startup, and t_Q is the time of full-power operation. Times are in days. Equation (10) is assumed to apply for all times later than 30 seconds past shutdown, that is, after delayed neutrons have become negligible.

Integration of equation (10) from 30 seconds after shutdown to time t yields an expression for the afterheat energy per unit reactor power. By applying the necessary conversion factors, including a coolant enthalpy rise of 15 (megawatts)(sec)/lb, the integrated equation gives afterheat-coolant weight per unit reactor power:

$$\frac{W_{AH}}{Q} = 44\left[(t - t_Q)^{0.8} - t^{0.8} + (t_Q + 0.000347)^{0.8} - 0.00171\right] \quad (11)$$

Again, times are in days and W_{AH}/Q is in pounds per megawatt.

In the 30-second time interval between shutdown and the point at which equations (10) and (11) become applicable, the power will fall off rapidly with time. However, the coolant ejected in the first 30 seconds will produce a considerable amount of thrust and should not be charged off as a total loss. The 30-second-coolant weight required is nearly proportional to reactor power when specific impulse is constant. For example, a continuous-thrust system with an initial thrust-weight ratio of 0.5 requires approximately 16.7 times as much afterheat coolant in this 30-second interval as would the same vehicle with F/W_G equal to 0.03. A perigee-propulsion spacecraft with an F/W_G of 0.03 would have the same 30-second-coolant requirement as the continuous-thrust system of the same initial acceleration, but this coolant expenditure would be required following each power-on period. As a result, the total requirement for the perigee-propulsion system would be nearer that of the $F/W_G = 0.5$ vehicle than to the $F/W_G = 0.03$ continuous-thrust example.

A quantitative estimate of coolant expenditure during the 30 seconds following shutdown can be made by assuming the power to decline linearly with time. The worst case, that of 0.5 initial acceleration with continuous thrust, would require only about 2.5 percent of the propulsion-period-propellant weight to provide the 30-second cooling, for a mission with a hyperbolic velocity of 3 miles per second and a specific impulse of 800 pounds per pound per second. Such a coolant weight would not be prohibitive even if it were wasted.

Since the first 30 seconds after shutdown may be considered part of the propulsion period, the afterheat-coolant-weight penalty will be the value obtained from equation (11). To be conservative, the integration may be carried out to infinite time after shutdown. When the same example is used and the comparison is made at the operating conditions used previously, equation (11) leads to the conclusion that thrust-to-initial-weight ratio and thrust-programing technique have little effect on afterheat-coolant weight. The effects of power level and power-on time, parameters nearly inversely proportional for a given mission, are such that W_{AH} is calculated to be between 1.5 and 2.5 percent of total propellant weight. Again, such a weight penalty is not prohibitive, and

perigee propulsion is not indicated to be significantly worse in this respect than continuous thrust. More refined calculations are not expected to alter these overall conclusions.

Application Aspects

The primary advantage of perigee propulsion over continuous-thrust propulsion is shown to be a reduction in required thrust-weight ratio. Either a specified vehicle weight can be propelled by a powerplant of lower thrust or a given powerplant can be used in a larger spacecraft when perigee propulsion is utilized. The overall worth of these changes is difficult to determine quantitatively and beyond the scope of this report. However, three aspects of the situation deserve consideration.

One important aspect of perigee propulsion application is the flexibility which is given to an existing powerplant. A comparison of figures 13(a) and (b) reveals that the optimum power for a 50,000-pound vehicle using continuous thrust is almost identical to the optimum power for a 500,000-pound spacecraft using perigee propulsion. Table I would indicate that separately optimized powerplants would have different flow areas and pressures, but these parameters have only secondary effects on residual load. Identical powerplants could be used in the two vehicles with essentially the same result as shown in figure 13. Use of perigee propulsion to various degrees would greatly enhance the utility of a nuclear-rocket powerplant.

The second noteworthy aspect is the opportunity to use powerplants of such low power that they would be impractical with continuous thrust. If particular powerplant types prove to be exceptionally light in weight or simple in design or fabrication at low powers, these advantages may be realized through use of perigee propulsion. Logical applications would be solar probes or other small vehicles.

The third benefit of perigee propulsion is indicated in table I, where optimum power density Q/v is shown to diminish as power is reduced. Although the values of pressure and flow area could be altered at a specified power level so as to reduce the power density somewhat, the trend in power density with power would remain. Since fuel-element heat flux and thermal stress are approximately proportional to power density, many development problems may be simplified by the opportunity to minimize reactor power.

Operational Considerations

Substitution of perigee propulsion for continuous thrust would entail several changes in the operational requirements and characteristics

of a nuclear-rocket spacecraft. Not all changes are detrimental. Four ways in which the thrust program would alter the situation are discussed: (1) by drastically changing the escape trajectory, (2) by requiring frequent variations in reactor power, (3) by subjecting the vehicle to longer times in the Van Allen radiation belts, and (4) by changing the ground rules which determine optimum powerplant staging.

A change in trajectory would be felt primarily in the requirements imposed on the navigation and control system. For a perigee-propulsion vehicle these requirements would be to determine thrust initiation and termination times, provide the desired thrust orientation during powered flight, and make all necessary corrections to keep the craft on a satisfactory trajectory. In some respects navigation and control in a low-thrust vehicle may be easier than in a high-thrust vehicle. Times available for position and path determination are greater, and the magnitude of the thrust is such that large errors will not arise unless small deviations are allowed to accumulate. Furthermore, path correction at apogee is relatively economical. Although no analysis has been made, the flight control of a perigee-propulsion system does not appear to be more difficult than that of a higher thrust vehicle.

Powerplant control for perigee propulsion would differ from that for continuous thrust only in the number of power cycles required. Initial startup in the parking orbit would be identical for the two schemes and would involve large changes in both reactor power and temperature. Subsequent power cycles in the perigee-propulsion thrust program would be primarily changes in power, because temperatures could probably be kept high during the intermediate coasting periods by careful regulation of afterheat-coolant flow. All power changes must be accompanied by precisely controlled propellant flow to prevent transient temperature overshoots. Once this capability has been built into the powerplant control system, the switch to perigee propulsion only means more frequent exercise of the capability. Reliability might suffer, but any mission requiring startup at Mars would have much more stringent requirements if the same control system were to be used.

Temperature cycling may be a more serious problem than power or flow variation. Many proposed reactor fuel-element or moderator materials are brittle and have little resistance to thermal stress. If a reactor has a required lift of only one temperature cycle, great simplification in design may be possible. However, staging of reactors will not be advantageous for all missions, and restart capability is likely to be a mandatory or highly desirable specification for a practical nuclear-rocket powerplant. Perigee-propulsion would require frequent temperature cycles of some extent, but the seriousness of this requirement is minimized by the expectation that overcooling by afterheat coolant can be prevented. In addition, and of more importance than the number of cycles required during a mission, development of a reliable

nuclear-rocket powerplant will require large numbers of ground tests. Consequently, the reactor must be designed to withstand temperature cycling in order to reduce the number of reactors required in a development program. Use of many one-shot reactors would be extremely expensive. If temperature cycling is made possible to meet the latter needs, this operational characteristic of perigee propulsion will not be serious.

The amount of shielding required to protect astronauts from the various forms of electromagnetic and particle radiations encountered in the space environment is not completely predictable at present. Solar flares and cosmic radiation may be equalizing factors that make total mission time the parameter of importance (ref. 10). Shield weights imposed by Van Allen belt radiation are indicated to exceed those for solar flare protection only for very low acceleration vehicles. Since perigee propulsion may present a problem in this respect, a comparison of thrust programs is made based on calculations of exposure times. Reference 11 indicates that continuous-thrust vehicles, starting from initial orbits of about 400-statute-mile altitude, would spend 2.5, 15, 180, or 1400 hours in the Van Allen belts for accelerations in initial orbit of 10^{-1}, 10^{-2}, 10^{-3}, or 10^{-4} g, respectively. These values, being for a specific impulse of about 7700 pounds per pound per second, are a little higher than corresponding times for nuclear rockets, but the difference would probably be less than 25 percent.

By means of a simplified analysis, order of magnitude exposure times for perigee-propulsion trajectories have been estimated. Assuming that travel time in the altitude ranges from 1000 to 3000 and 8000 to 12,000 miles is equivalent to time in the radiation belts, the analysis indicates that perigee-propulsion systems with initial acceleration of 0.03 and 0.01 g would have exposure times of about 12 and 36 hours, respectively. If only time in the inner belt is important, lower but roughly proportional times would be involved. By this comparison, the Van Allen belt shielding problem for a manned nuclear rocket utilizing perigee propulsion would be intermediate between that of (1) a 0.5-g continuous-thrust system, which would traverse the belts in an hour or two, and (2) an electrical-propulsion spacecraft, which would require protection for about 2 months. Interpolation between the data in reference 10 indicates that the shield weight for a 1-day passage would be considerably less than that for protection from a giant solar flare. Short flights, where protection is required from only major solar flares, would not be likely to profit from perigee propulsion.

The previously discussed possibility of reducing reactor weight has a further implication in the operational application of the perigee-propulsion principle: Powerplant staging may not be required. Whenever a reduction in reactor flow area will result in a significantly

lower powerplant weight, as is the case for combinations of high pressure and large flow area, powerplant staging will be advantageous. For example, an Earth-Mars round trip might be best accomplished with three or four reactors carried in separate stages that could be discarded. Each successive planetary escape or capture would be accomplished with a reactor of appropriate flow area, that is, a reactor capable of producing optimum thrust-weight ratio for the particular stage. However, since perigee propulsion results in reductions in operating pressure and powerplant weight, the desirability of powerplant staging will be diminished or removed entirely.

CONCLUSIONS

The principal conclusions of the perigee-propulsion analysis are summarized by the following. (A discussion of other aspects of the concept is found in the preceding text.)

1. For values of specific impulse and thrust-to-initial-weight ratio typical of orbital-launch nuclear rockets and for hyperbolic velocities representative of attractive interplanetary flight paths, perigee propulsion offers an interesting compromise between mass ratio and time to reach desired energy. By applying thrust over trajectory segments subtending central angles of about 60° to 120°, mass ratios approaching impulsive values can be achieved without causing total time to reach prohibitive magnitudes.

2. Preliminary comparisons of perigee propulsion and continuous thrust for Earth-Mars probe missions, taking into account estimated variations of specific impulse, hyperbolic velocity, powerplant weight, and tank weight, indicate that comparable performance can be achieved with large differences in required reactor power. For equal residual-load capability perigee-propulsion reactor powers are lower by an order of magnitude. The power reduction may be as high as a factor of 20 or more for minimum-energy paths and would probably be no less than 7 for any Earth-Mars mission. This advantage of perigee propulsion could be utilized to reduce the reactor power for a given vehicle or increase the stage weight for a given powerplant.

Lewis Research Center
National Aeronautics and Space Administration
Cleveland, Ohio, August 31, 1961

APPENDIX - SYMBOLS

A_f reactor flow area, sq ft

E vehicle energy per unit mass, $(\text{miles/sec})^2$

F thrust, lb

g_c gravitational constant, 32.174 ft/sec^2

H enthalpy, (megawatts)(sec)/lb

h altitude, statute miles

I specific impulse, lb/(lb/sec)

P hydrogen pressure, lb/sq in. abs

Q reactor power, megawatts

r radius from center of Earth, statute miles

t time, sec (unless otherwise specified)

V reactor volume, cu ft

v velocity, miles/sec

Δv impulsive velocity increment, ft/sec

W weight, lb

α angle between velocity vector and local horizontal, deg

β angle between thrust and velocity vectors, deg

θ central angle (see fig. 2), deg

$\Delta\theta$ central angle between point on trajectory and perigee of preceding coasting ellipse, deg

μ force constant of Earth, $\text{miles}^3/\text{sec}^2$

Subscripts:

AH afterheat

E empty

e	reactor exit
G	gross
h	hyperbolic
i	reactor inlet
n	perigee number
P	propellant
PP	powerplant
Q	full-power (operating time)
RL	residual load, eq. (8)
ST	structure
T	tank
t	total (time to reach desired energy)
vac	in vacuum
0	perigee
1	beginning of propulsion period
2	end of propulsion period

REFERENCES

1. Camac, Morton: Reduction of Flight Time and Propellant Requirements of Satellites with Electric Propulsion by the Use of Stored Electrical Energy. Preprint 721-58, Am. Rocket Soc., Inc., 1958.

2. Roberson, Robert E.: Time for Escape Using a Succession of Small Impulses. ARS Jour., vol. 29, no. 5, May 1959, pp. 370-371.

3. Moeckel, W. E.: Trajectories with Constant Tangential Thrust in Central Gravitational Fields. NASA TR R-53, 1960.

4. Moeckel, W. E.: Interplanetary Trajectories with Excess Energy. Proc. IX Int. Astronautical Cong., Amsterdam (Holland), 1958. Vol. I. Springer-Verlag, 1959, pp. 96-119.

5. Breakwell, John V., Gillespie, Rollin W., and Ross, Stanley: Researches in Interplanetary Transfer. Preprint 954-59, Am. Rocket Soc., Inc., 1959.

6. King, Charles R.: Compilation of Thermodynamic Properties, Transport Properties, and Theoretical Rocket Performance of Gaseous Hydrogen. NASA TN D-275, 1960.

7. Johnson, Paul G., and Smith, Roger L.: An Optimization of Powerplant Parameters for Orbital-Launch Nuclear Rockets. NASA TN D-675, 1961.

8. Himmel, S. C., Dugan, J. F., Jr., Luidens, R. W., and Weber, R. J.: A Study of Manned Nuclear-Rocket Missions to Mars. Paper 61-49, Inst. Aerospace Sci., Inc., 1961.

9. Glasstone, Samuel: Principles of Nuclear Reactor Engineering. D. Van Nostrand Co., Inc., 1955, p. 119.

10. Wallner, Lewis E., and Kaufman, Harold R.: Radiation Shielding for Manned Space Flight. Paper presented at IAS Nat. Flight Prop. Meeting, Cleveland (Ohio), Mar. 9-10, 1961.

11. Babinsky, Andrew D., Del Duca, Michael G., and Bond, Angus F.: The Radiation Problem in Low Thrust Space Travel. Preprint 989-59, Am. Rocket Soc., Inc., 1959.

TABLE I. - COMPARISON OF THRUST-PROGRAMING TECHNIQUES

(a) Gross weight, 500,000 pounds; reactor exit temperature, 4500° F; mission time, 209 days; reactor exit Mach number, 0.4

Thrust program	Continuous					Perigee propulsion			
F/W_G	0.01		0.03	0.10	0.50	0.01		0.03	0.05
Expansion process	Equilibrium	No dissociation	Equilibrium	Equilibrium	Equilibrium	Equilibrium	No dissociation	Equilibrium	Equilibrium
P_e, lb/sq in. abs	10	100	30	100	1000	10	100	30	40
I_{vac}, lb/(lb/sec)	955	878	920	898	878	955	878	920	913
A_f, sq ft	2.99	0.32	3.07	3.09	1.56	2.99	0.32	3.07	3.80
W_{PP}, lb	6500	4000	6800	7100	8000	6500	4000	6800	7800
W_{ST}, lb	10,000	10,000	10,000	10,000	10,000	10,000	10,000	10,000	10,000
t_t, days	~0	~0	~0	~0	~0	20	20	10	8
v_h, miles/sec	2.72	2.72	2.72	2.72	2.72	2.78	2.78	2.74	2.73
W_G/W_E	2.21	2.37	2.00	1.74	1.61	1.67	1.75	1.61	1.58
W_P, lb	273,800	289,000	250,000	212,500	189,500	200,000	213,500	189,500	182,500
W_T, lb	21,900	23,100	20,000	17,000	15,200	16,000	17,100	15,200	14,600
W_{RL}, lb	187,800	173,900	213,200	253,400	277,300	267,500	255,400	278,500	285,100
W_{RL}/W_G	0.376	0.348	0.426	0.507	0.555	0.535	0.511	0.557	0.570
Q, megawatts	124	118	357	1150	5500	124	118	357	580
Q/v, megawatts/cu ft	3.2	7.2	8.6	36.5	45.8	3.2	7.2	8.6	9.0

TABLE I. - Concluded. COMPARISON OF THRUST-PROGRAMING TECHNIQUES

(b) Gross weight, 50,000 pounds; reactor exit temperature, 4500° F; mission time, 209 days; reactor exit Mach number, 0.4

Thrust program	Continuous					Perigee propulsion			
F/W_G	0.01		0.03	0.10	0.50	0.01		0.03	0.05
Expansion process	Equilibrium	No dissociation	Equilibrium	Equilibrium	Equilibrium	Equilibrium	No dissociation	Equilibrium	Equilibrium
P_e, lb/sq in. abs	3	15	10	33	200	3	15	10	12
I_{vac}, lb/(lb/sec)	1015	878	955	917	891	1015	878	955	948
A_f, sq ft	0.96	0.22	0.90	0.92	0.78	0.96	0.22	0.90	1.25
W_{PP}, lb	4200	3800	4200	4300	4400	4200	3800	4200	4500
W_{ST}, lb	1000	1000	1000	1000	1000	1000	1000	1000	1000
t_t, days	~0	~0	~0	~0	~0	20	20	10	8
v_h, miles/sec	2.72	2.72	2.72	2.72	2.72	2.78	2.78	2.74	2.73
W_G/W_E	2.11	2.37	1.96	1.72	1.60	1.62	1.75	1.58	1.55
W_P, lb	26,300	28,900	24,400	20,900	18,800	19,100	21,300	18,400	17,700
W_T, lb	2100	2300	2000	1700	1500	1500	1700	1500	1400
W_{RL}, lb	16,500	13,800	18,500	22,100	24,300	24,200	22,000	25,000	25,400
W_{RL}/W_G	0.330	0.276	0.370	0.442	0.486	0.484	0.440	0.500	0.508
Q, megawatts	13	13	37	118	567	13	13	37	62
Q/v, megawatts/cu ft	0.6	0.8	1.9	5.9	29.1	0.6	0.8	1.9	2.7

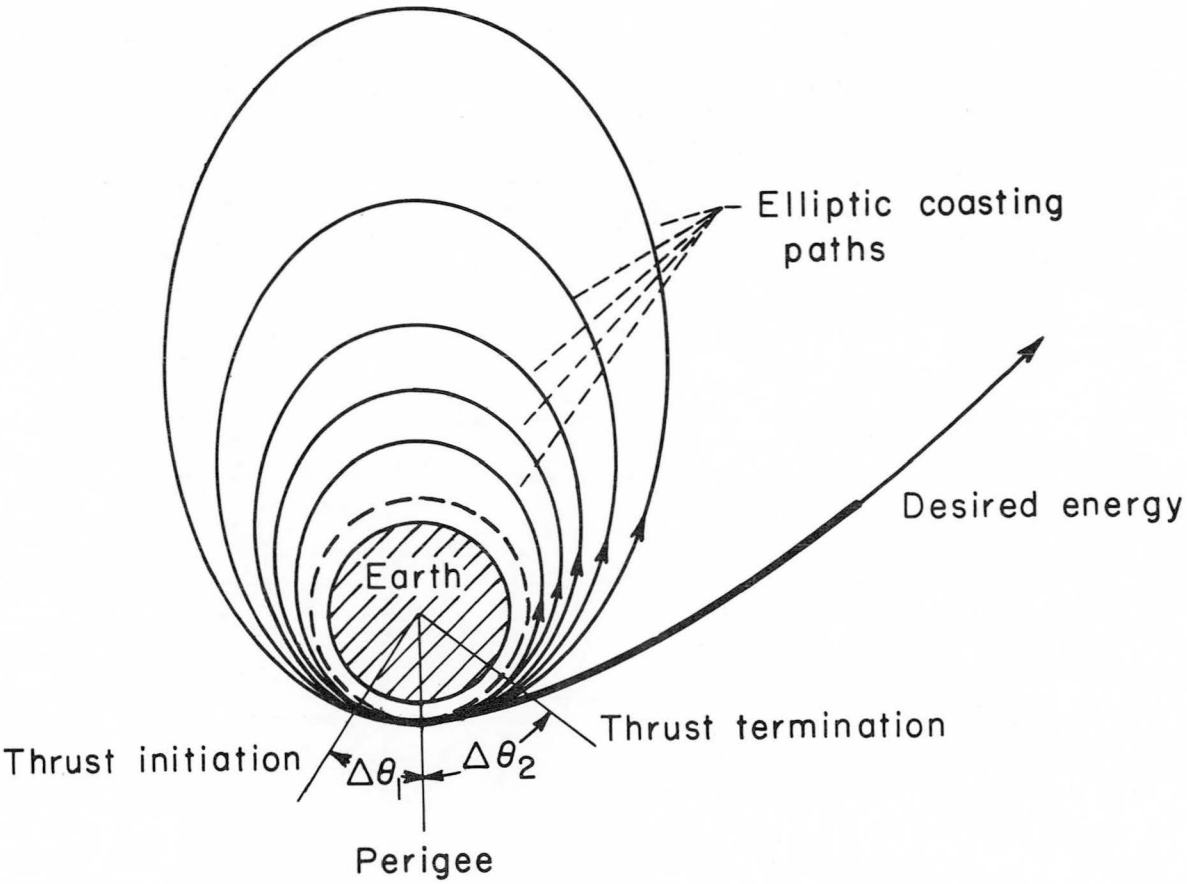

Figure 1. - Perigee-propulsion trajectory. Changes in perigee altitude and angular position neglected.

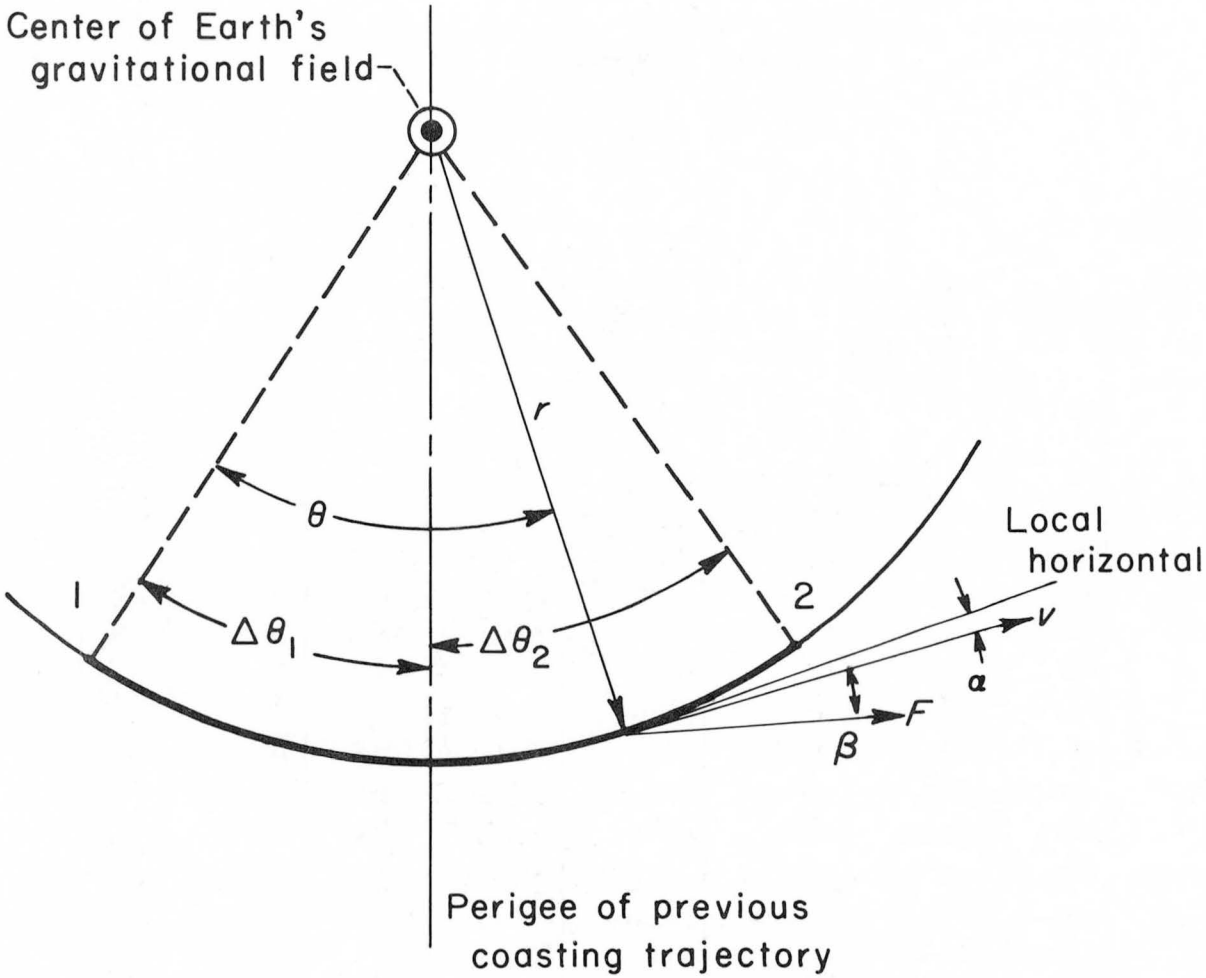

Figure 2. - Nomenclature and conventions for powered flight.

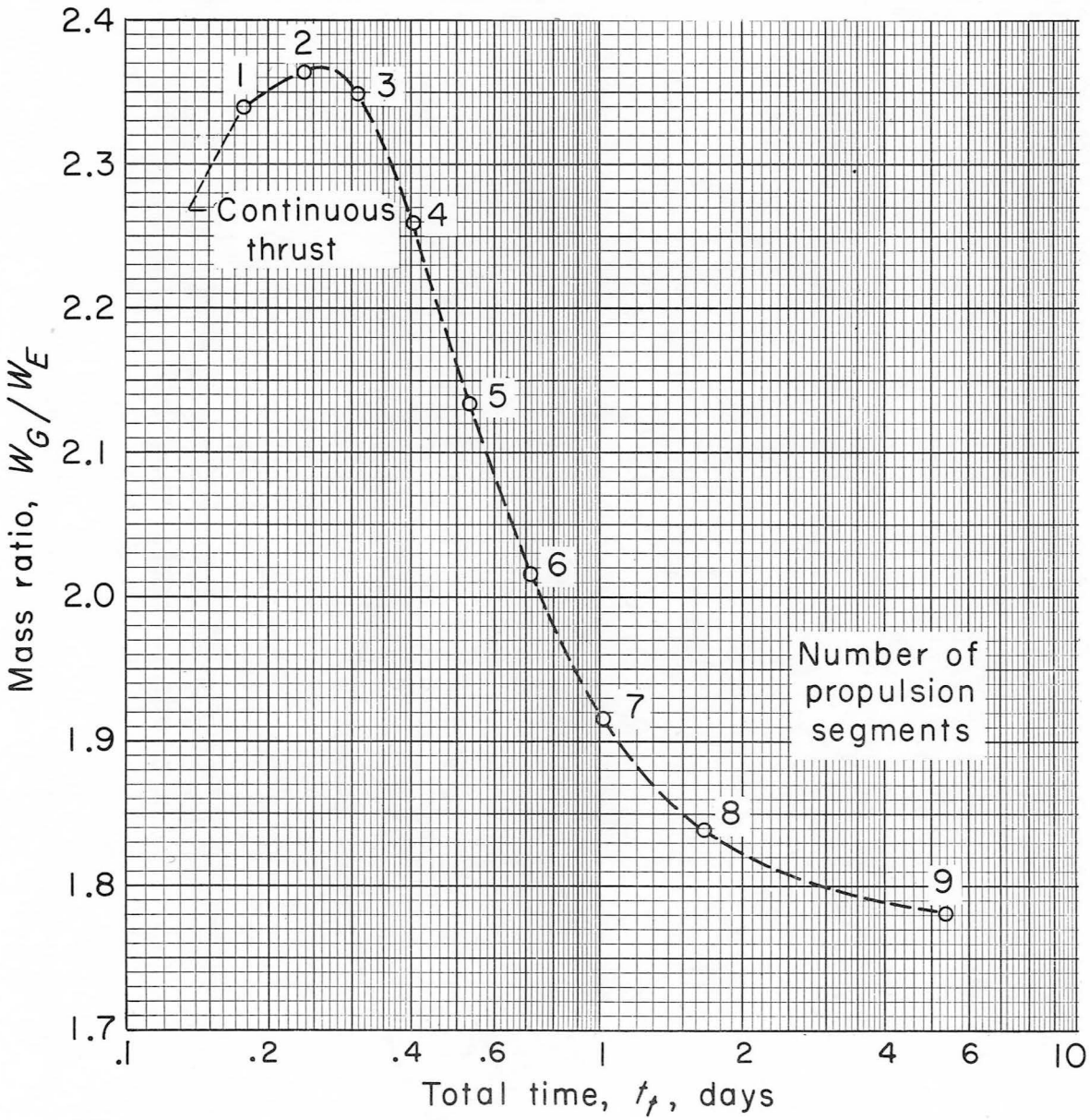

Figure 3. - Typical perigee-propulsion performance. Specific impulse, 800 pounds per pound per second; thrust-weight ratio, 0.03; hyperbolic velocity, 3 miles per second; β, 0°; $\Delta\theta_1$, 45°; $\Delta\theta_2$, 30°.

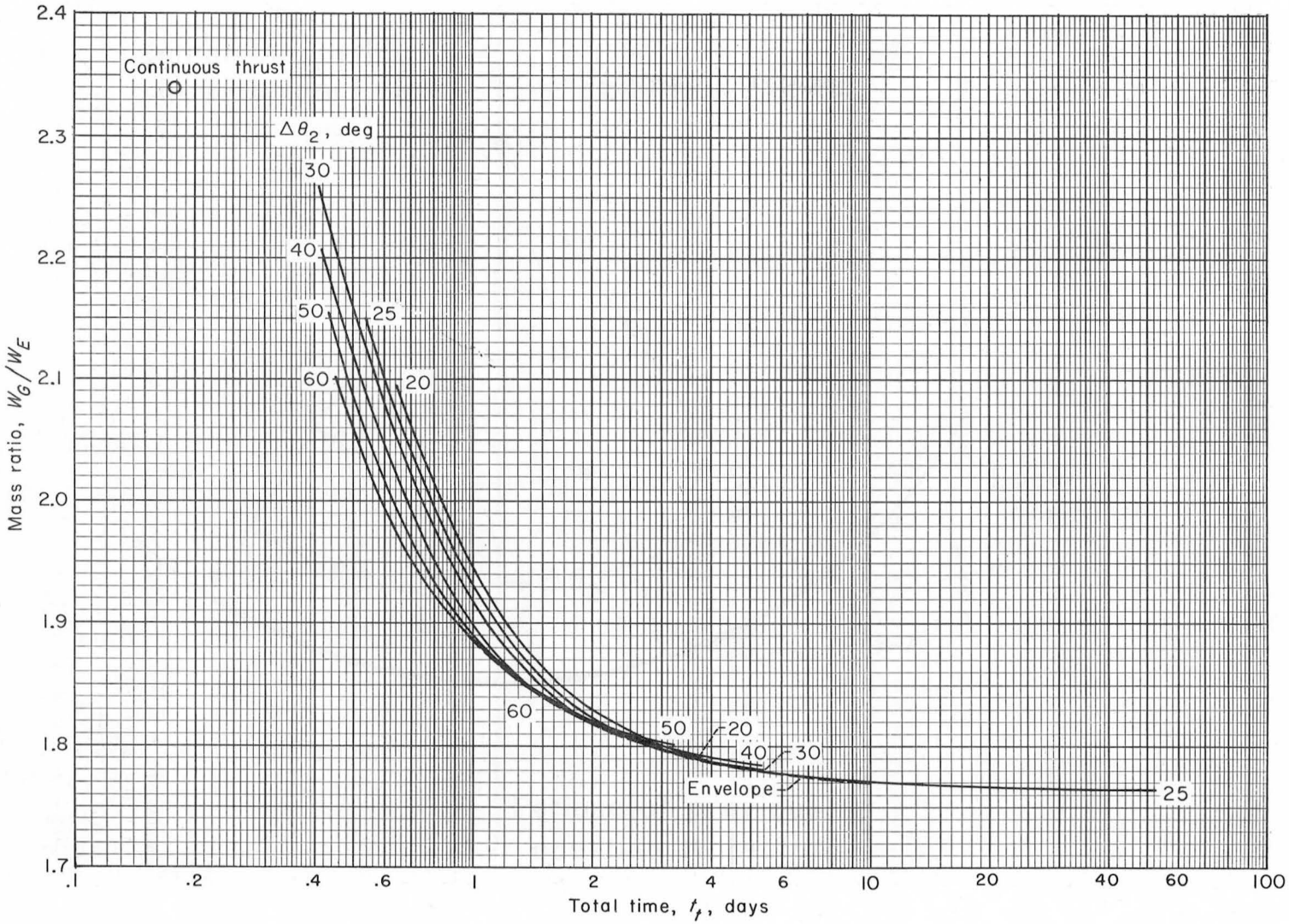

Figure 4. - Optimization of $\Delta\theta_2$. Specific impulse, 800 pounds per pound per second; thrust-weight ratio, 0.03; hyperbolic velocity, 3 miles per second; β, 0°; $\Delta\theta_1$, 45°.

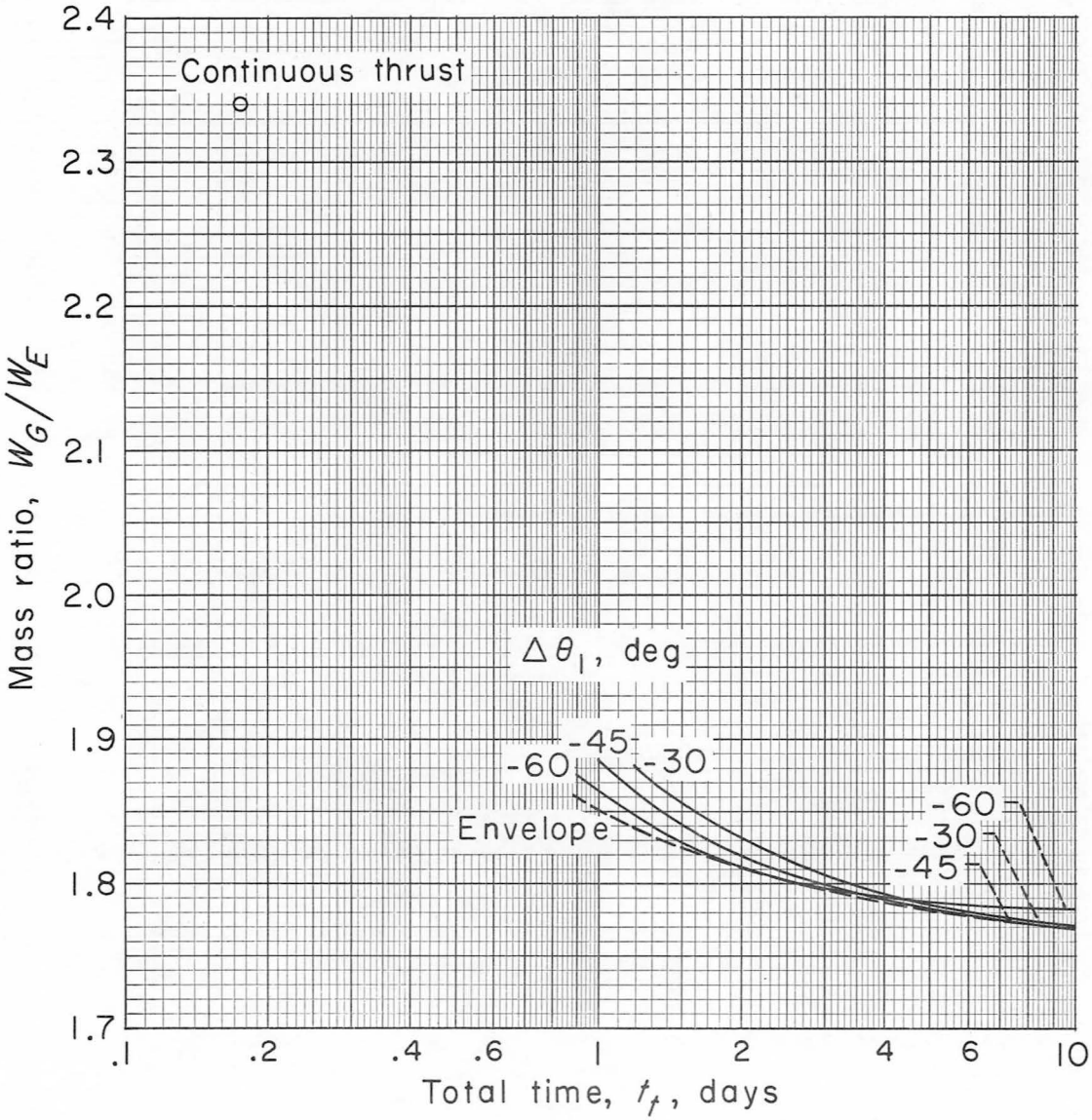

Figure 5. - Optimization of $\Delta\theta_1$. Specific impulse, 800 pounds per pound per second; thrust-weight ratio, 0.03; hyperbolic velocity, 3 miles per second; β, 0°; optimum $\Delta\theta_2$.

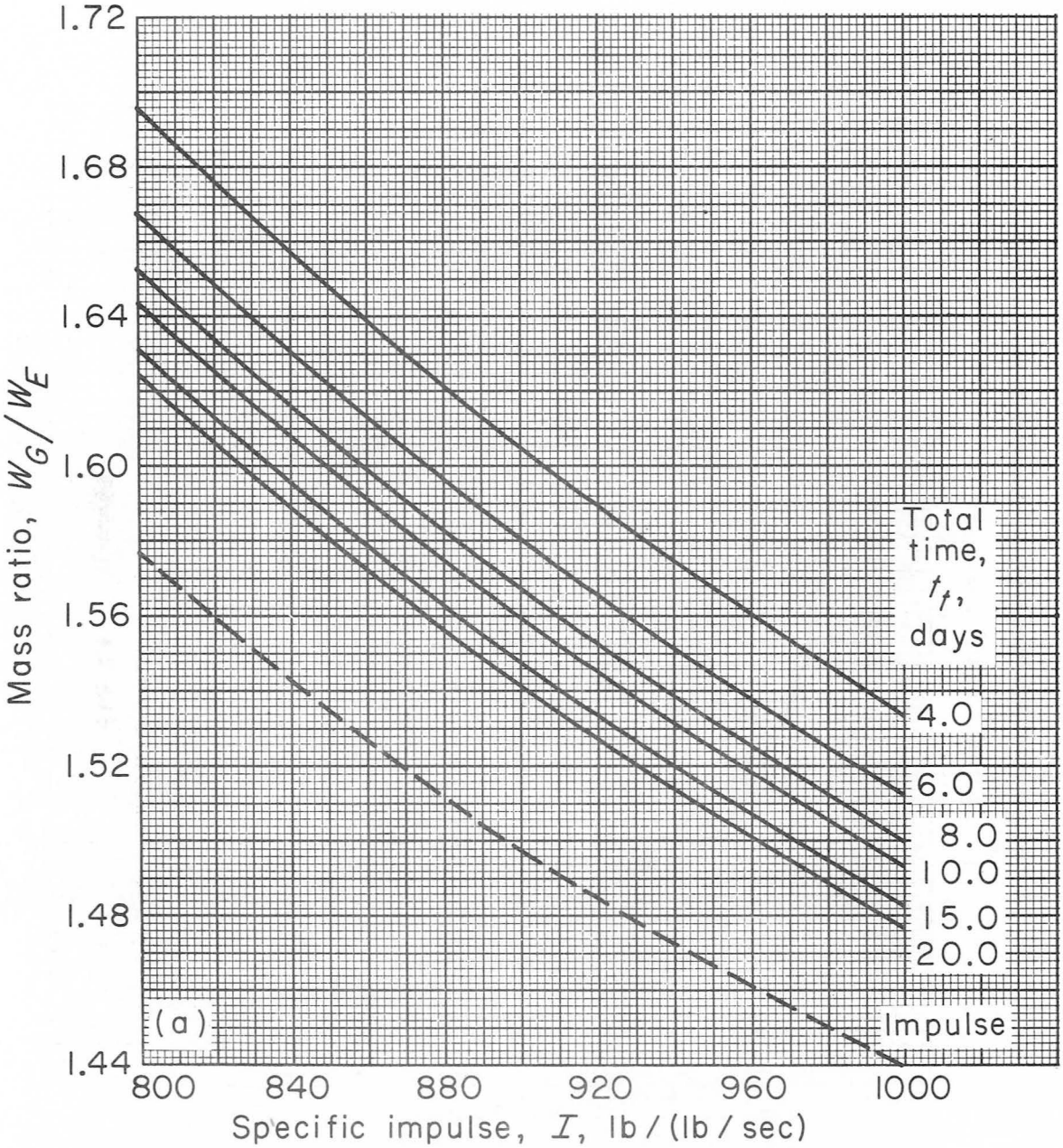

(a) Thrust-weight ratio, 0.01; hyperbolic velocity, 1.855 miles per second.

Figure 6. - Variation of mass ratio with specific impulse. β, 0°; optimum $\Delta\theta_1$ and $\Delta\theta_2$.

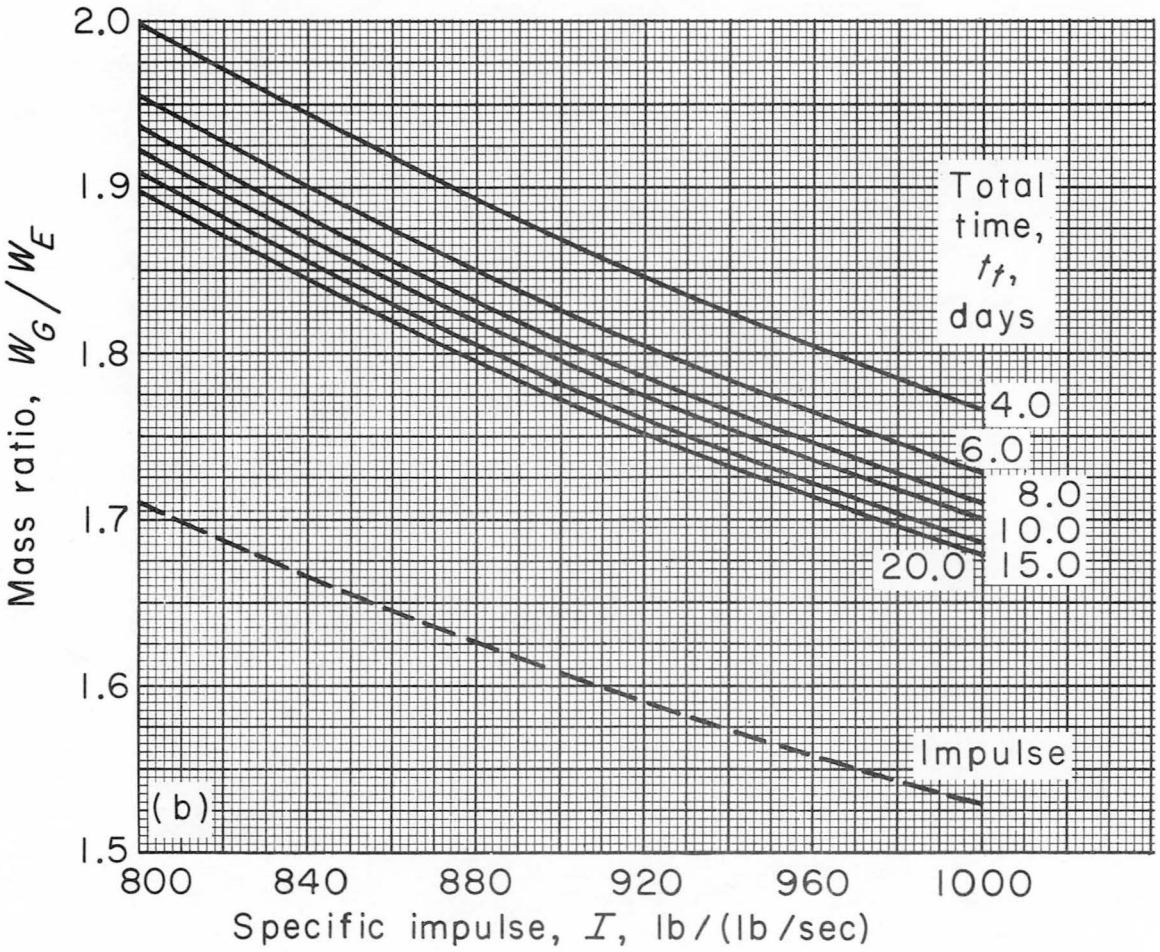

(b) Thrust-weight ratio, 0.01; hyperbolic velocity, 3.0 miles per second.

Figure 6. - Continued. Variation of mass ratio with specific impulse. β, 0°; optimum $\Delta\theta_1$ and $\Delta\theta_2$.

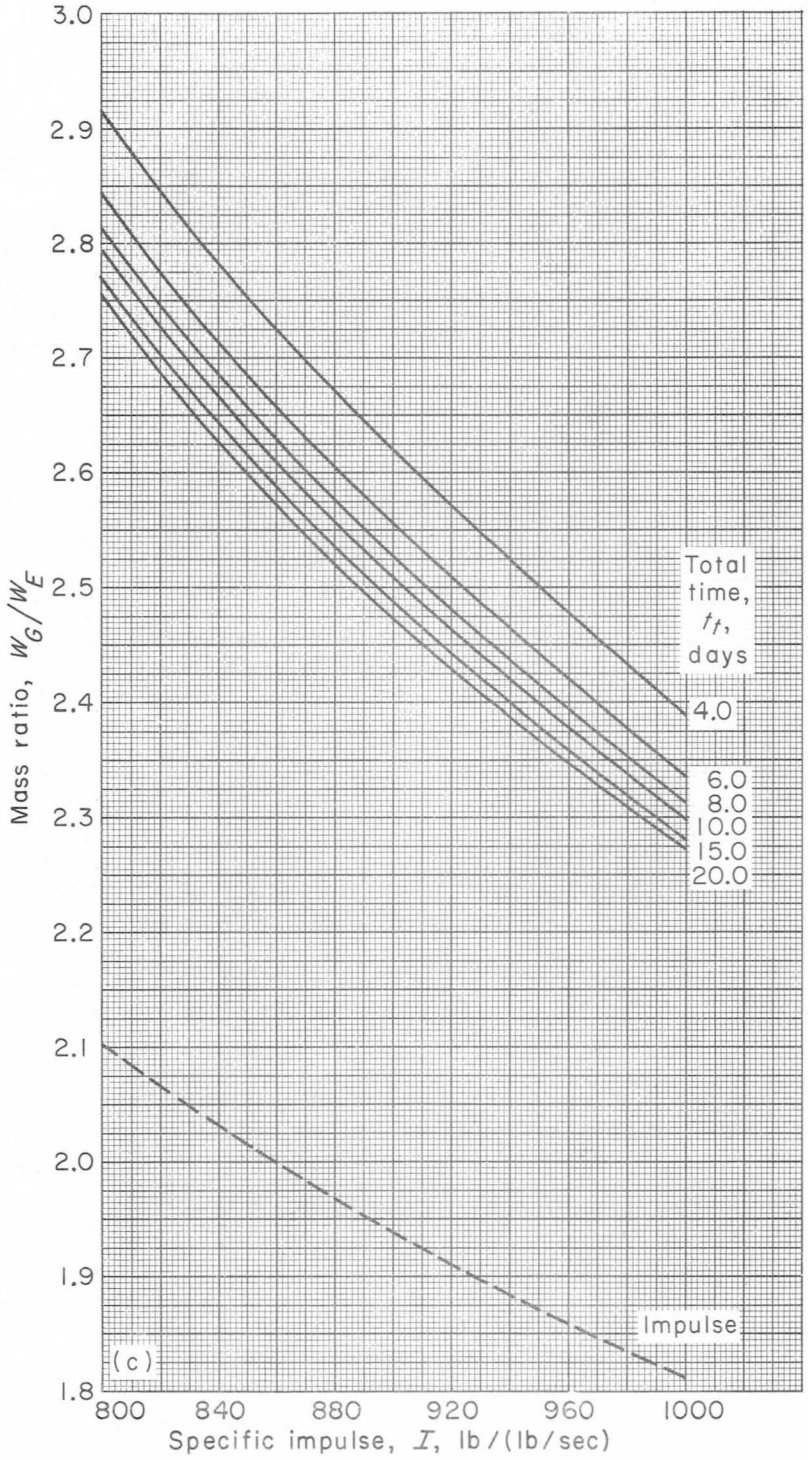

(c) Thrust-weight ratio, 0.01; hyperbolic velocity, 5.0 miles per second.

Figure 6. - Continued. Variation of mass ratio with specific impulse. β, 0°; optimum $\Delta\theta_1$ and $\Delta\theta_2$.

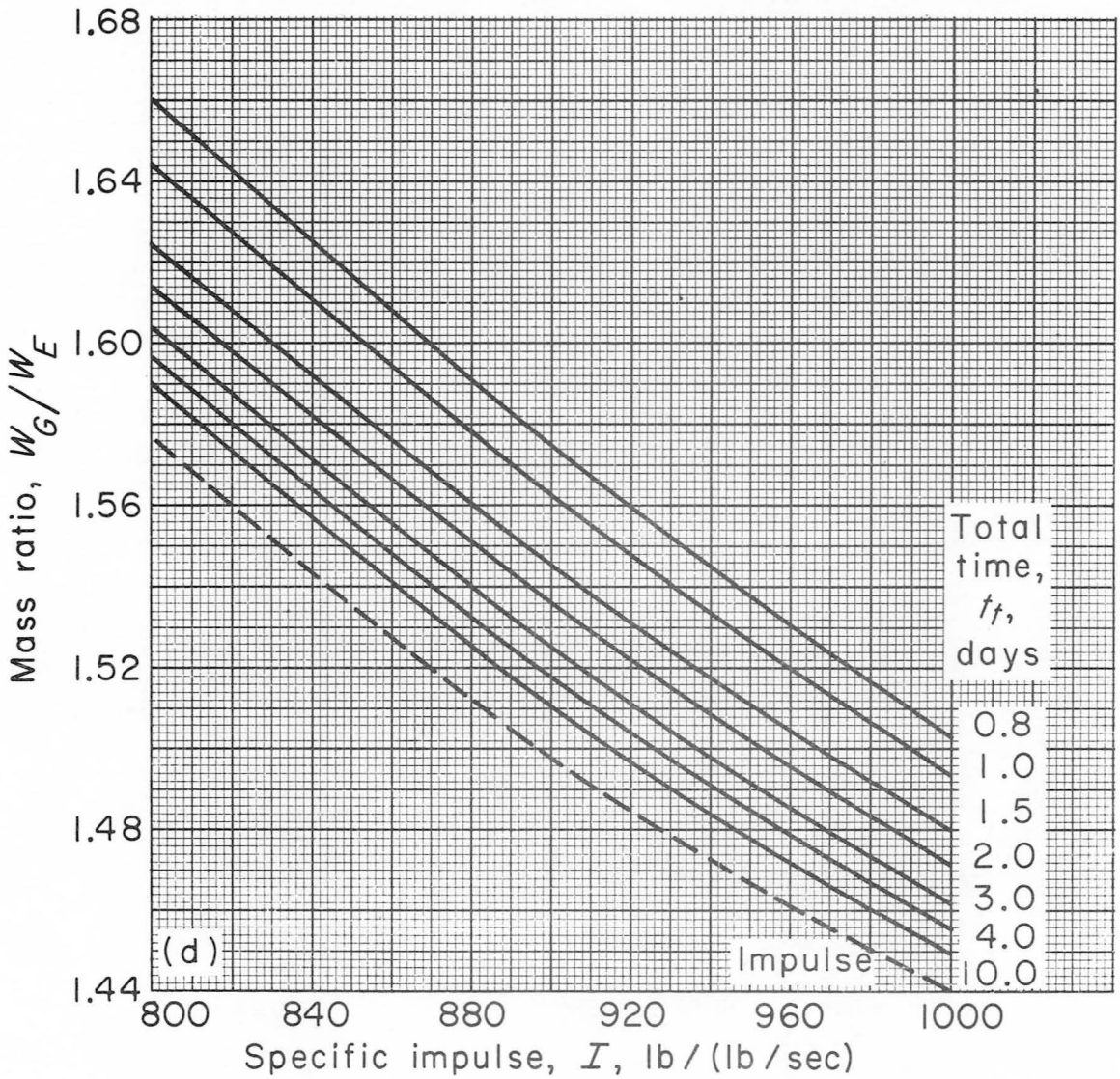

(d) Thrust-weight ratio, 0.03; hyperbolic velocity, 1.855 miles per second.

Figure 6. - Continued. Variation of mass ratio with specific impulse. β, 0°; optimum $\Delta\theta_1$ and $\Delta\theta_2$.

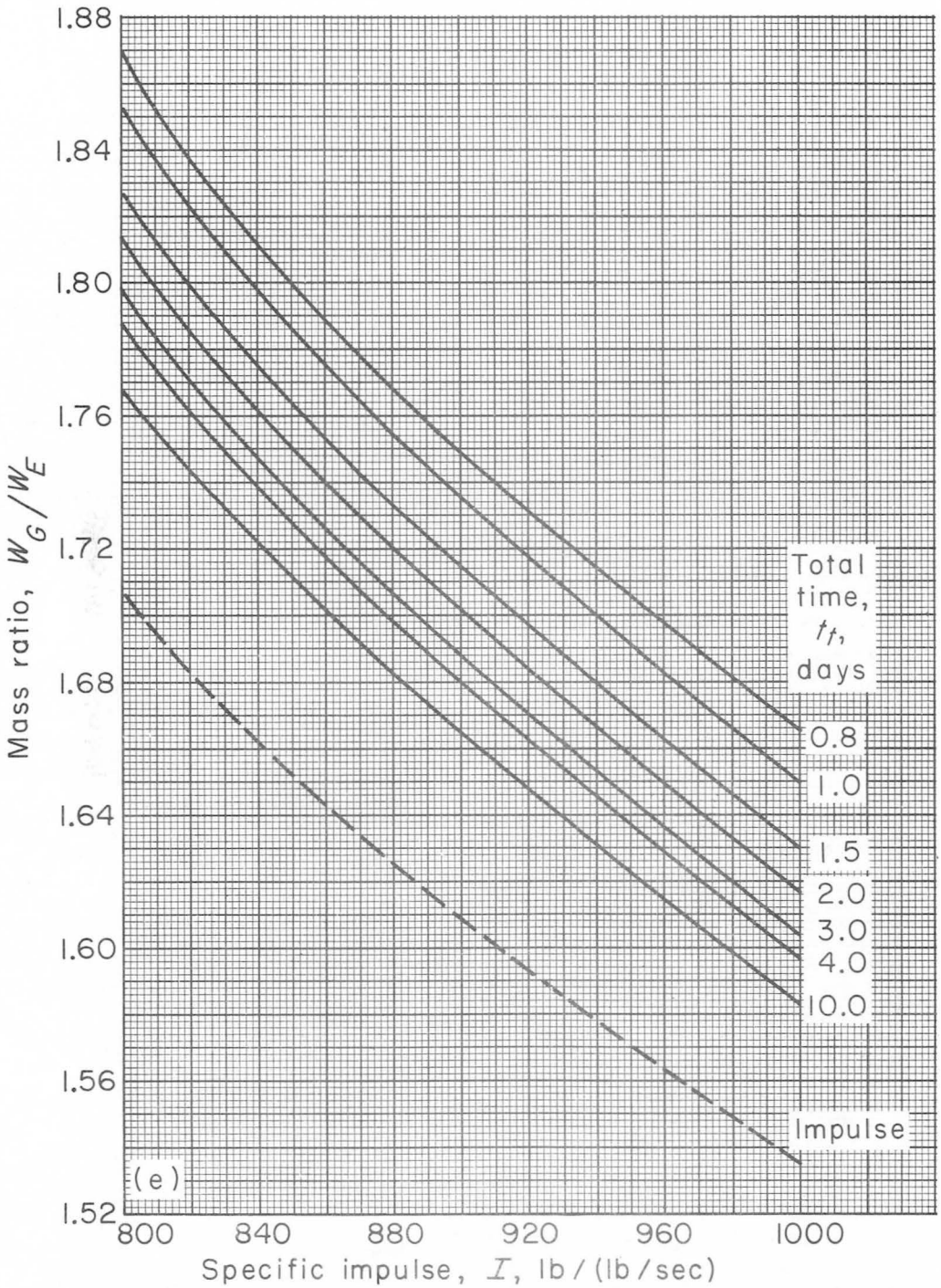

(e) Thrust-weight ratio, 0.03; hyperbolic velocity, 3.0 miles per second.

Figure 6. - Continued. Variation of mass ratio with specific impulse. β, 0°; optimum $\Delta\theta_1$ and $\Delta\theta_2$.

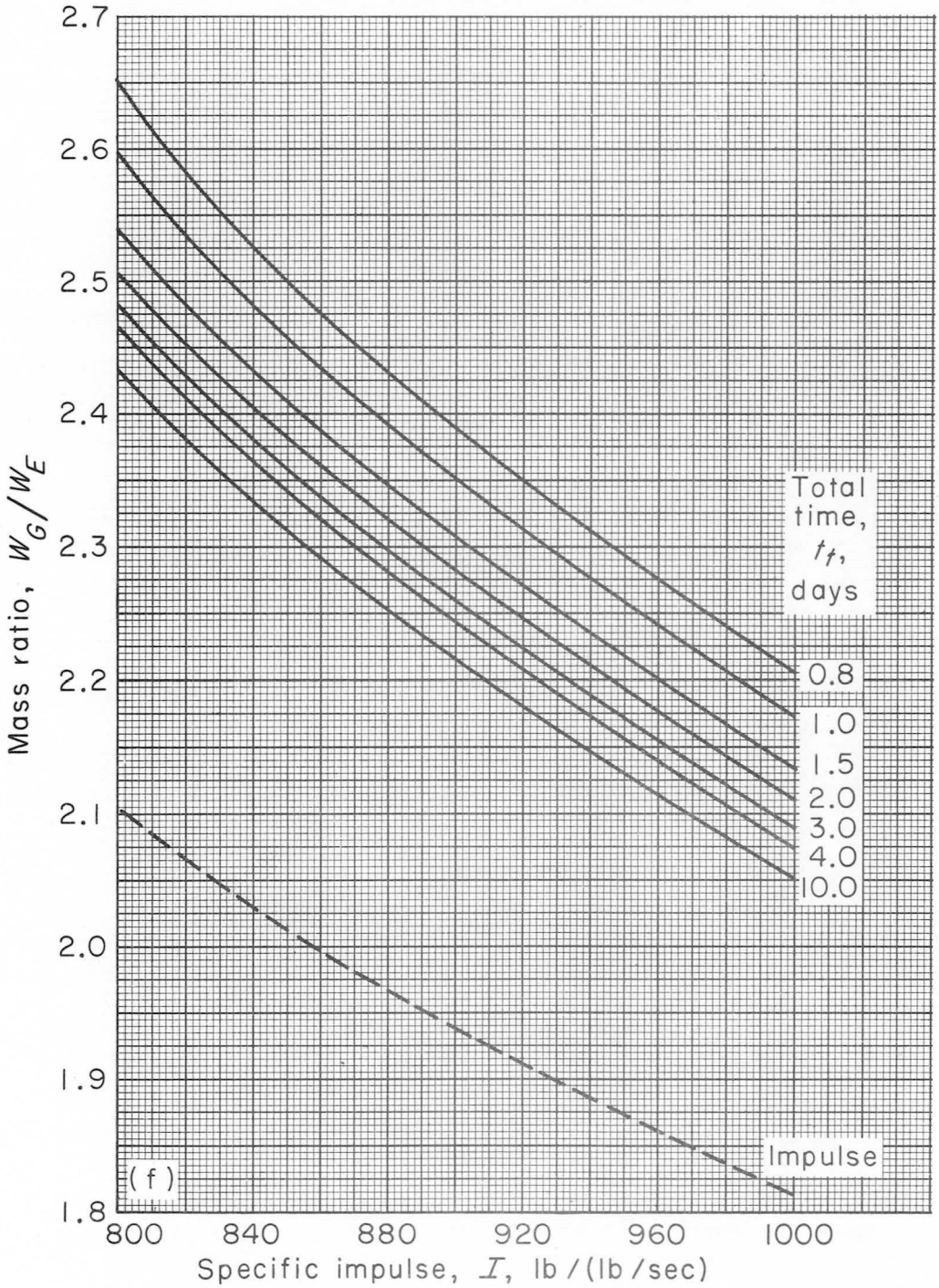

(f) Thrust-weight ratio, 0.03; hyperbolic velocity, 5.0 miles per second.

Figure 6. - Continued. Variation of mass ratio with specific impulse. β, 0°; optimum $\Delta\theta_1$ and $\Delta\theta_2$.

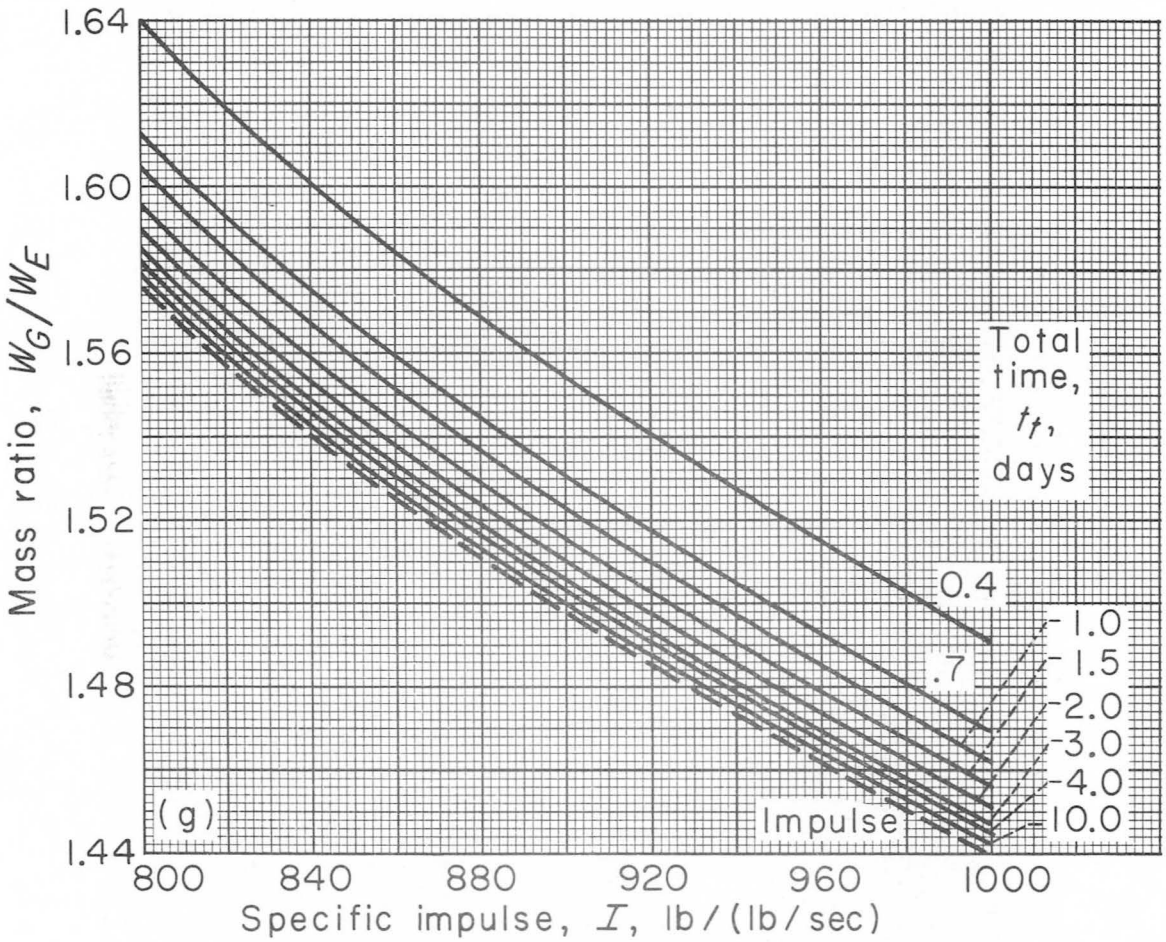

(g) Thrust-weight ratio, 0.05; hyperbolic velocity, 1.855 miles per second.

Figure 6. - Continued. Variation of mass ratio with specific impulse. β, 0°; optimum $\Delta\theta_1$ and $\Delta\theta_2$.

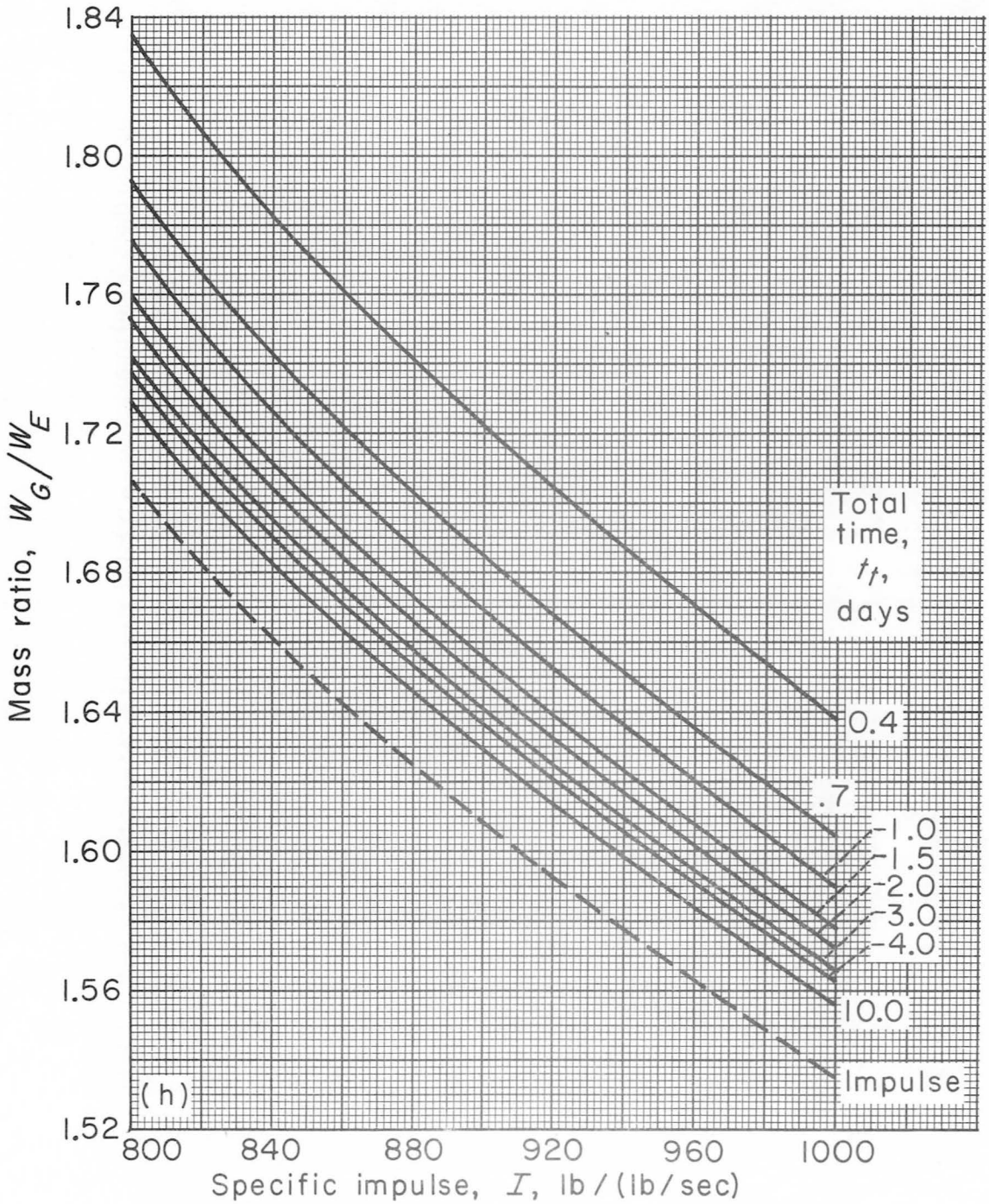

(h) Thrust-weight ratio, 0.05; hyperbolic velocity, 3.0 miles per second.

Figure 6. - Continued. Variation of mass ratio with specific impulse. β, 0°; optimum $\Delta\theta_1$ and $\Delta\theta_2$.

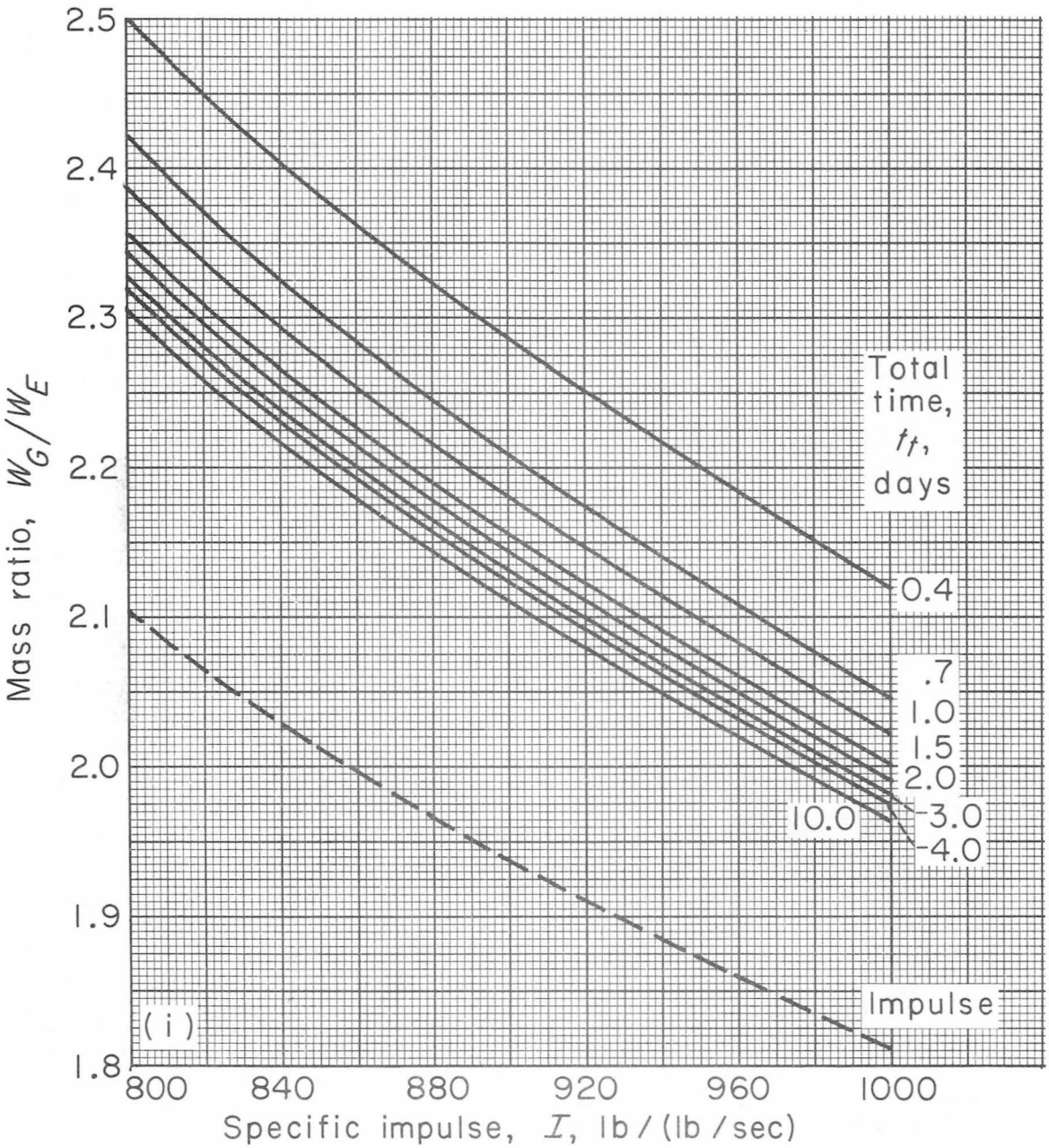

(i) Thrust-weight ratio, 0.05; hyperbolic velocity, 5.0 miles per second.

Figure 6. - Concluded. Variation of mass ratio with specific impulse. β, 0°; optimum $\Delta\theta_1$ and $\Delta\theta_2$.

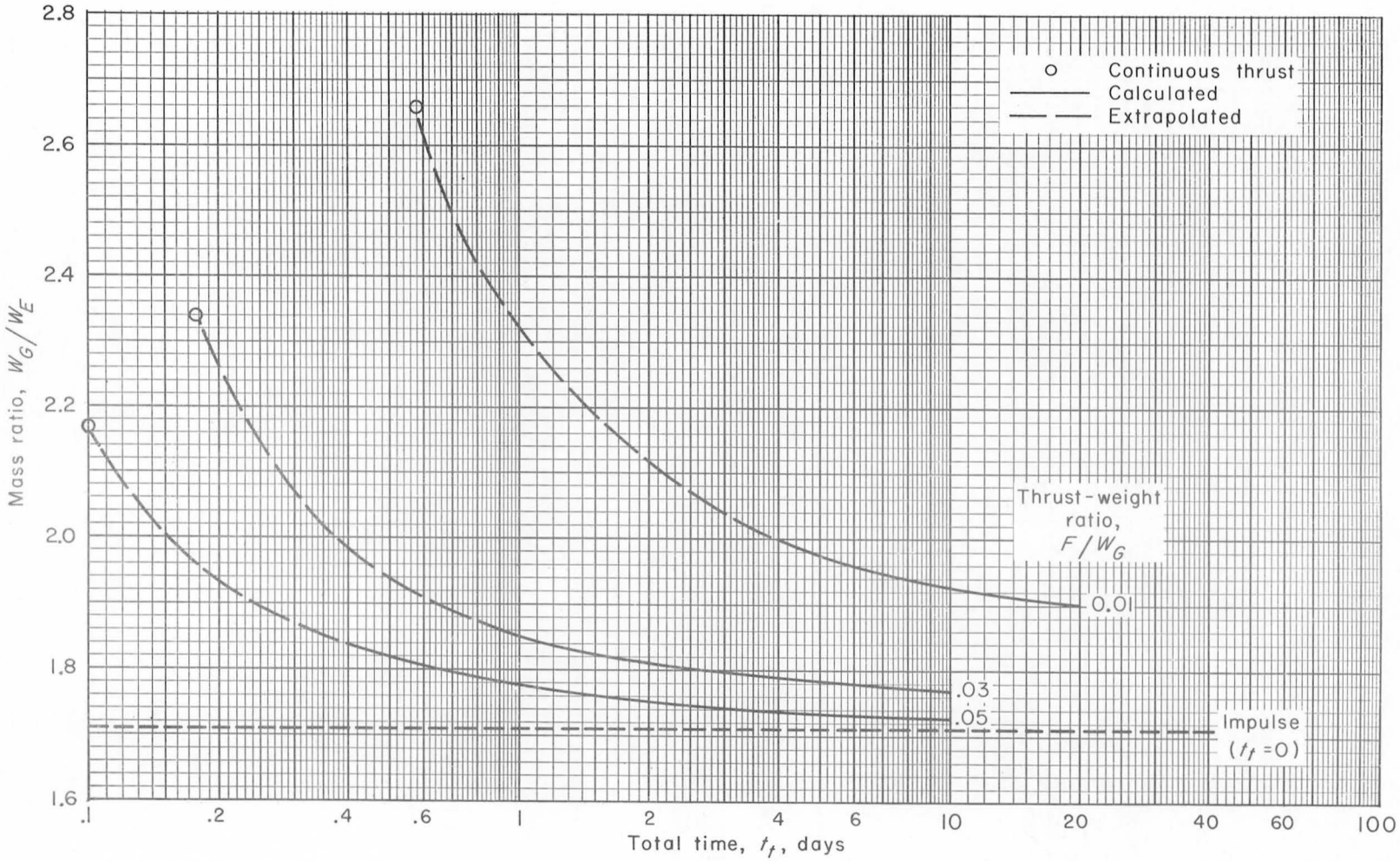

Figure 7. - Effect of thrust-weight-ratio variation. Specific impulse, 800 pounds per pound per second; hyperbolic velocity, 3.0 miles per second; β, 0°, optimum $\Delta\theta_1$ and $\Delta\theta_2$.

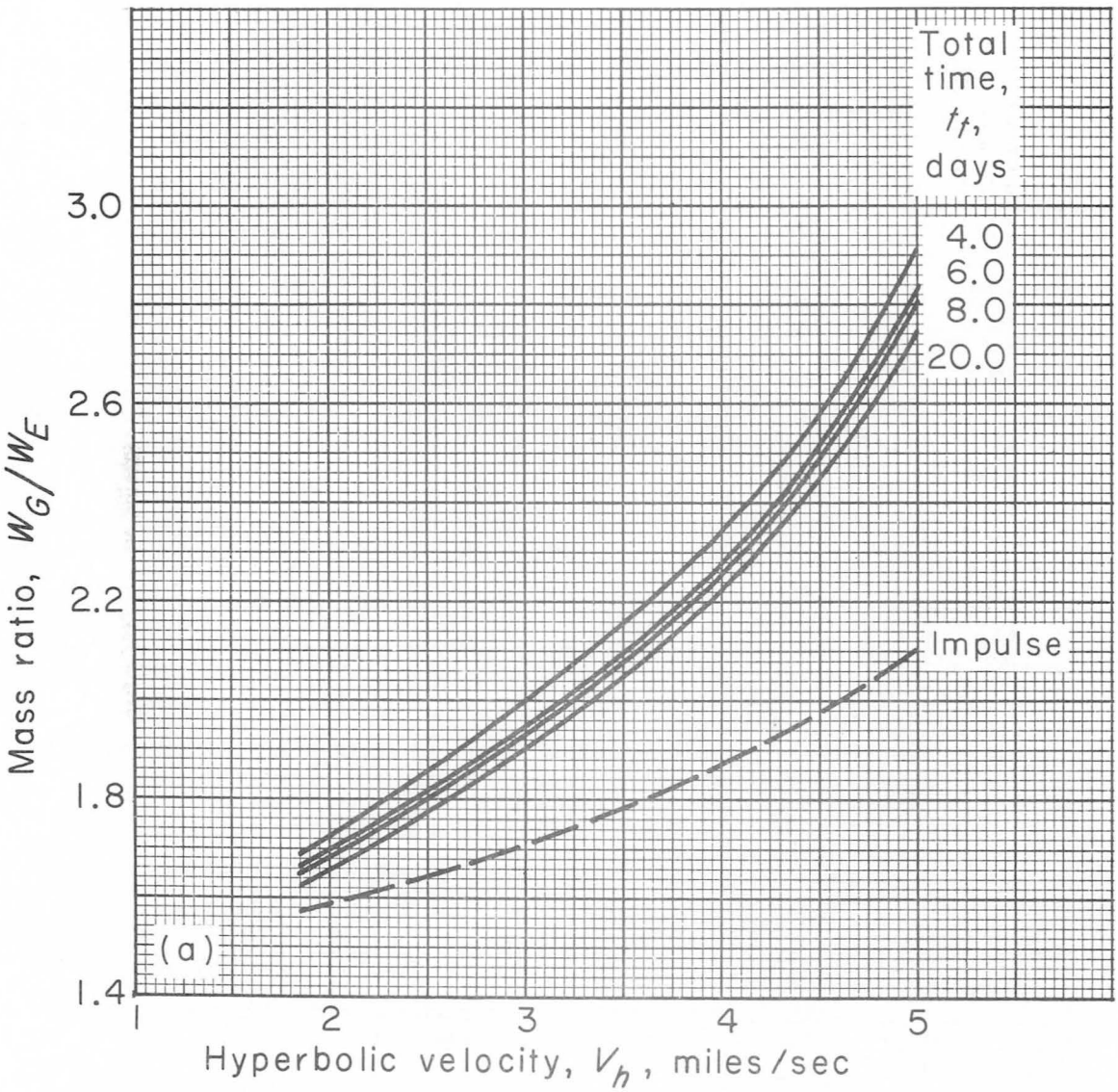

(a) Thrust-weight ratio, 0.01; specific impulse, 800 pounds per pound per second.

Figure 8. - Variation of mass ratio with hyperbolic velocity. β, 0°; optimum $\Delta\theta_1$ and $\Delta\theta_2$.

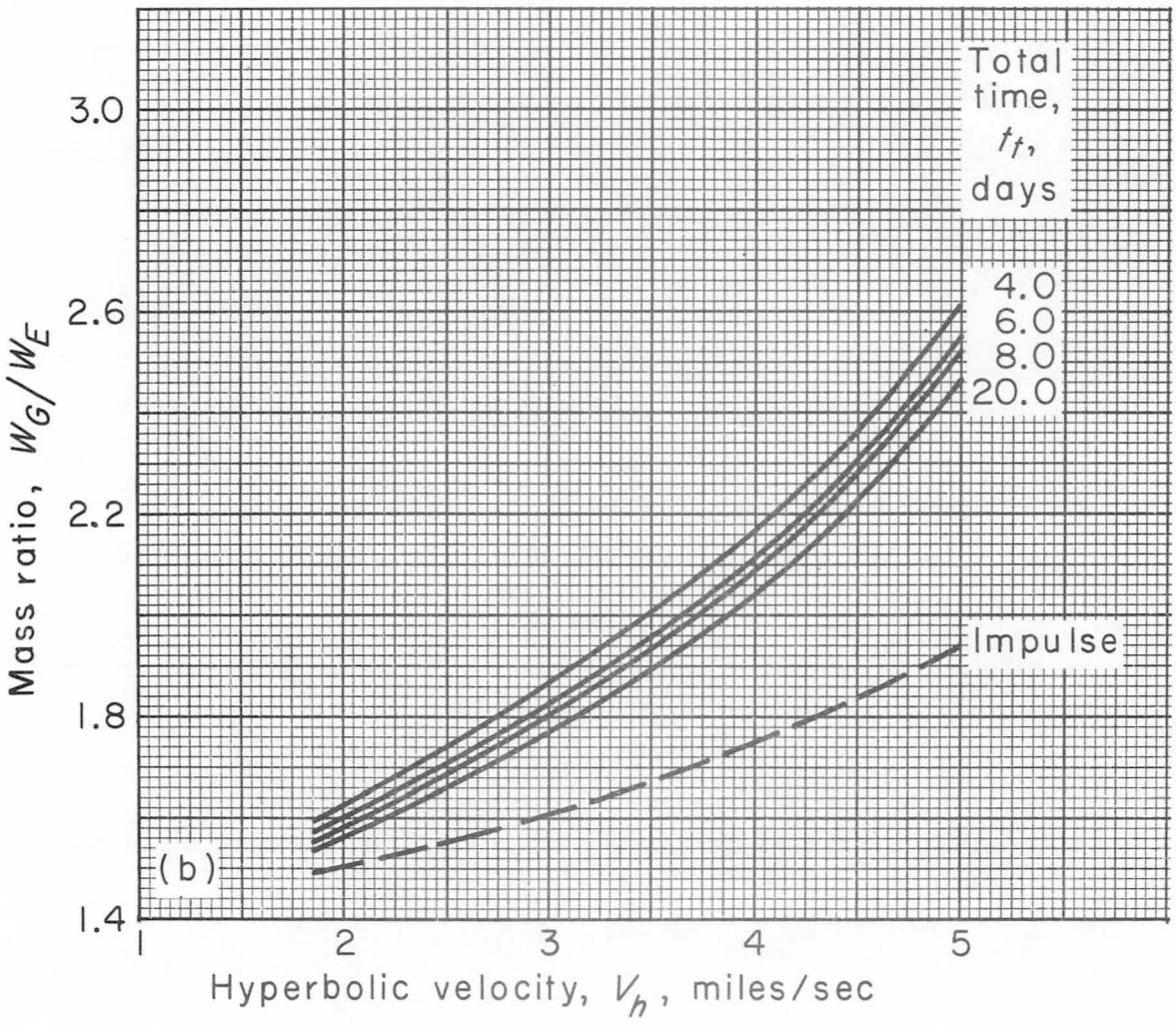

(b) Thrust-weight ratio, 0.01; specific impulse, 900 pounds per pound per second.

Figure 8. - Continued. Variation of mass ratio with hyperbolic velocity. β, 0°; optimum $\Delta\theta_1$ and $\Delta\theta_2$.

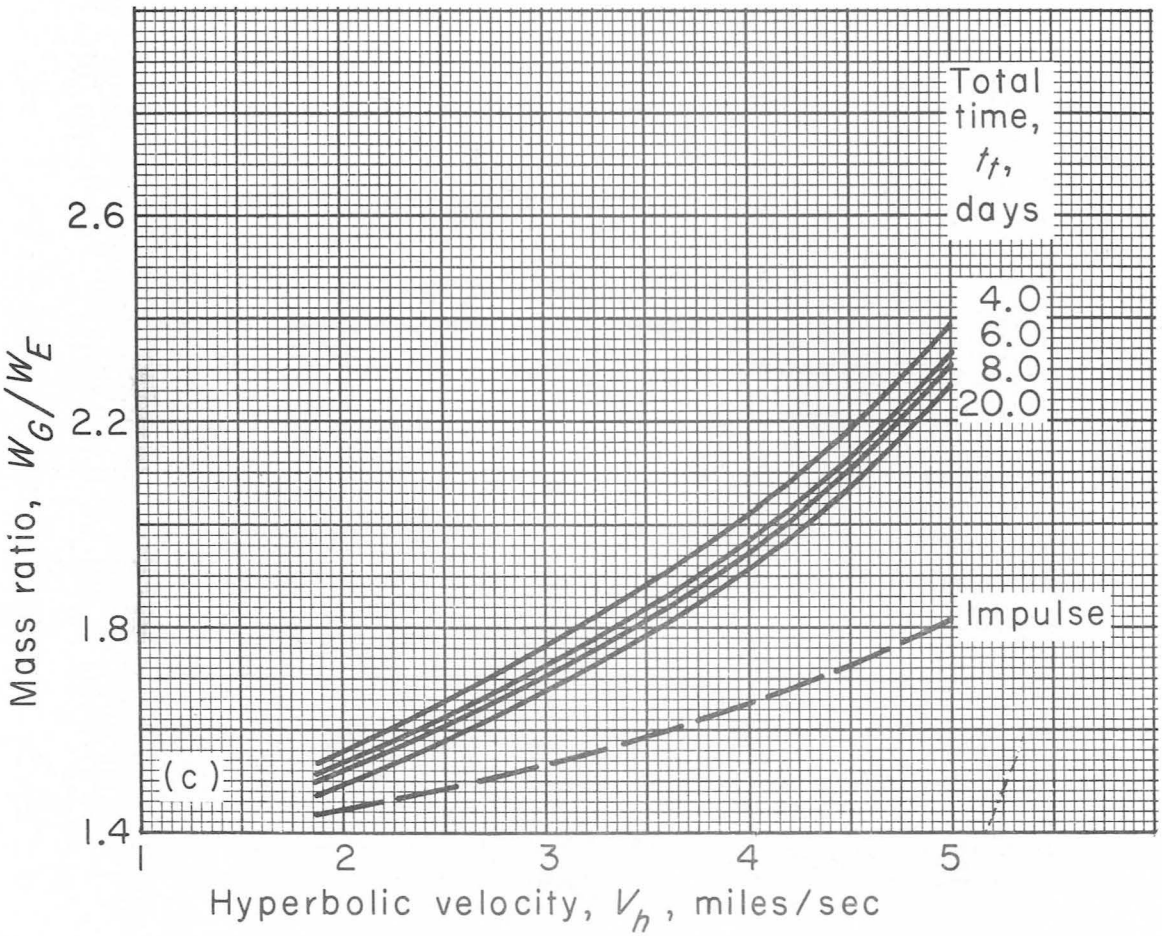

(c) Thrust-weight ratio, 0.01; specific impulse, 1000 pounds per pound per second.

Figure 8. - Continued. Variation of mass ratio with hyperbolic velocity. β, 0°; optimum $\Delta\theta_1$ and $\Delta\theta_2$.

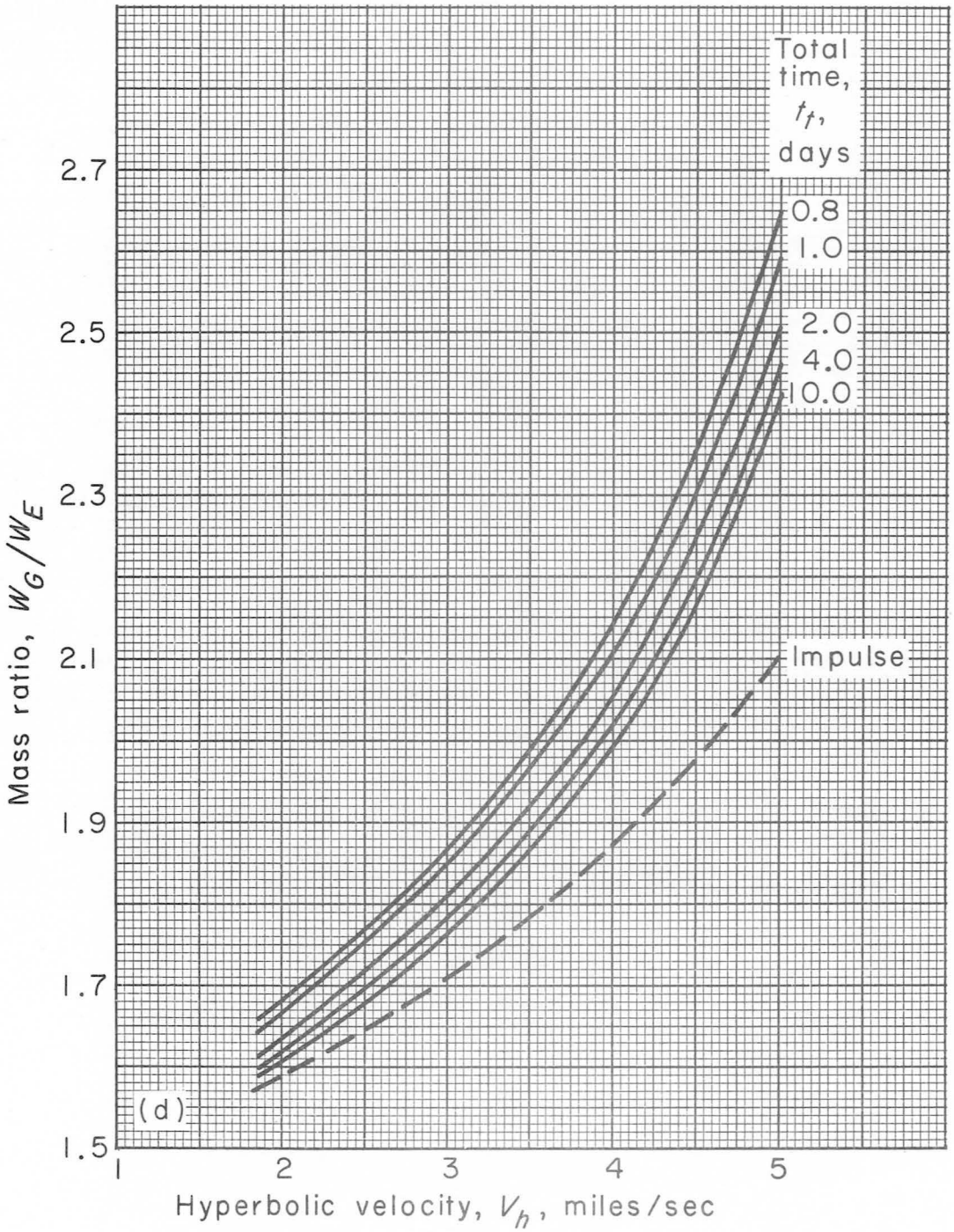

(d) Thrust-weight ratio, 0.03; specific impulse, 800 pounds per pound per second.

Figure 8. - Continued. Variation of mass ratio with hyperbolic velocity. β, 0°; optimum $\Delta\theta_1$ and $\Delta\theta_2$.

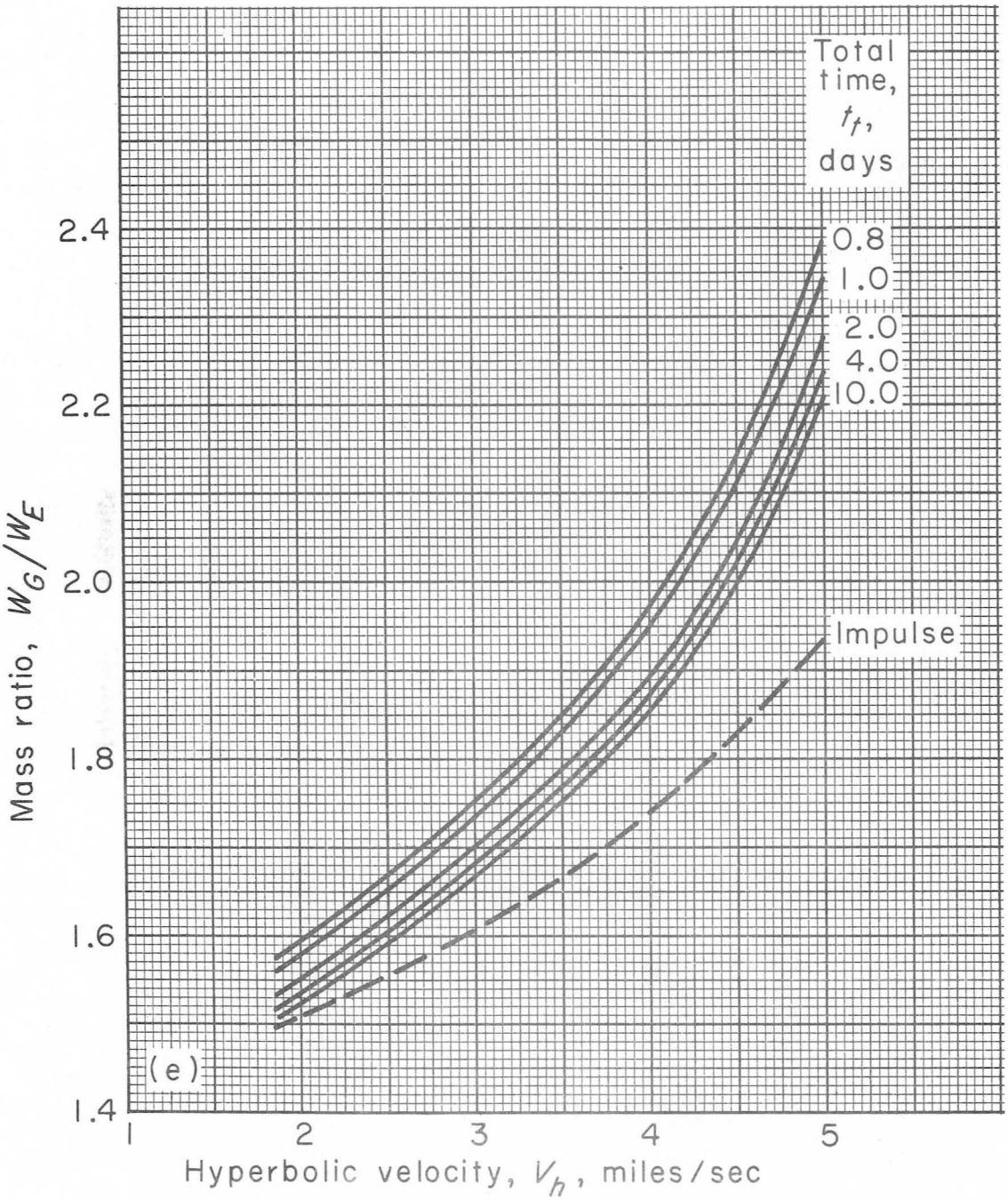

(e) Thrust-weight ratio, 0.03; specific impulse, 900 pounds per pound per second.

Figure 8. - Continued. Variation of mass ratio with hyperbolic velocity. β, 0°; optimum $\Delta\theta_1$ and $\Delta\theta_2$.

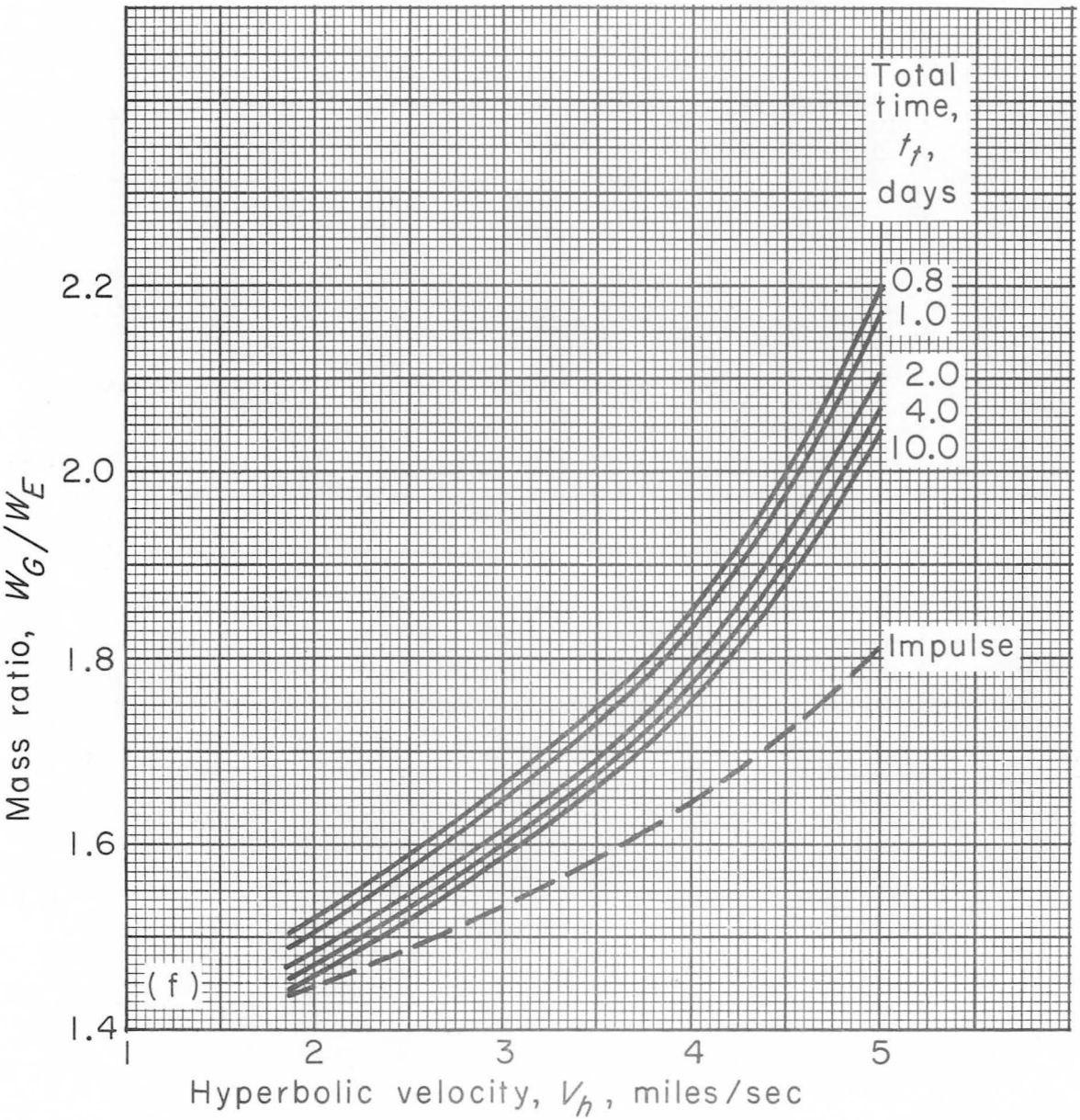

(f) Thrust-weight ratio, 0.03; specific impulse, 1000 pounds per pound per second.

Figure 8. - Continued. Variation of mass ratio with hyperbolic velocity. β, 0°; optimum $\Delta\theta_1$ and $\Delta\theta_2$.

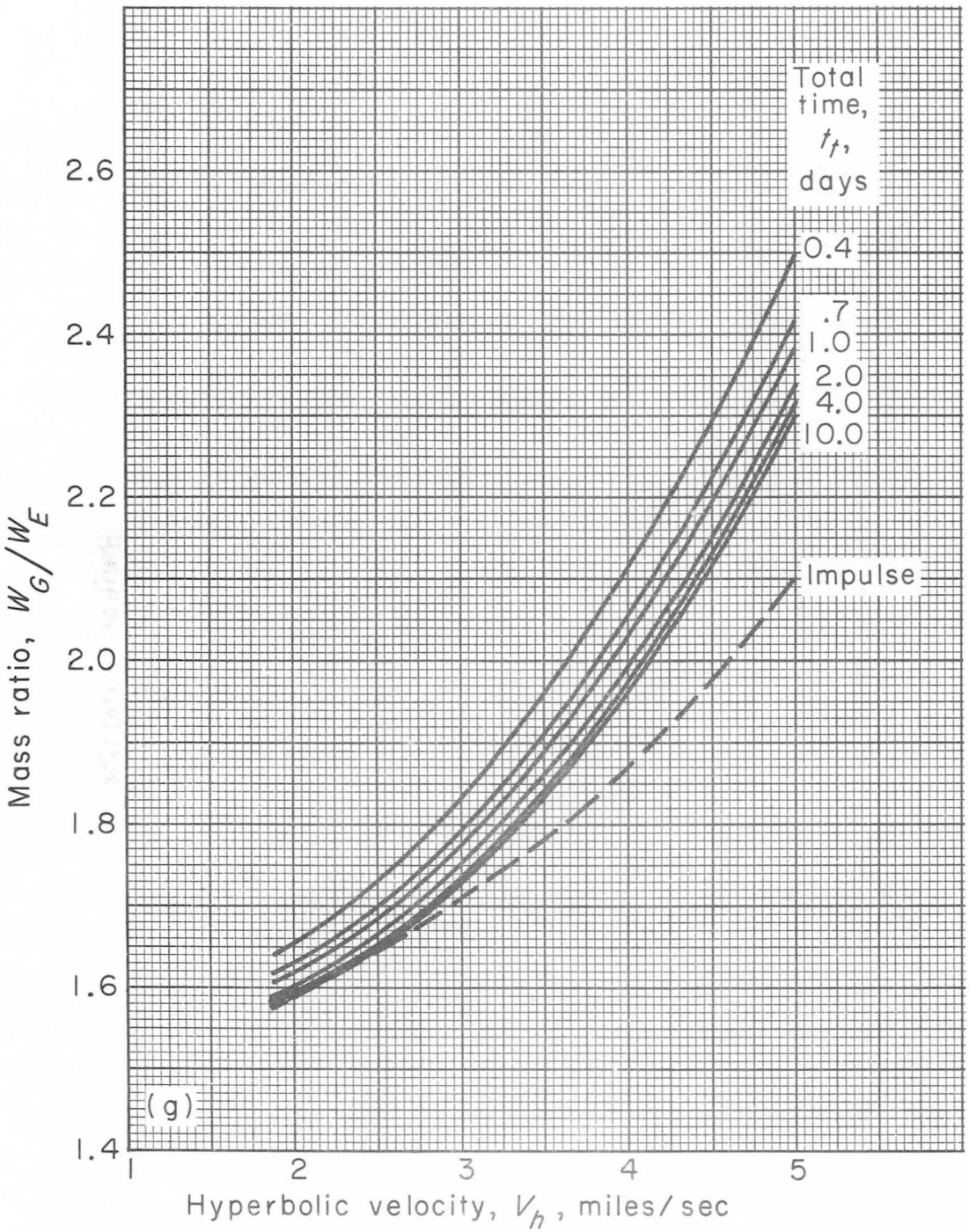

(g) Thrust-weight ratio, 0.05; specific impulse, 800 pounds per pound per second.

Figure 8. - Continued. Variation of mass ratio with hyperbolic velocity. β, 0°; optimum $\Delta\theta_1$ and $\Delta\theta_2$.

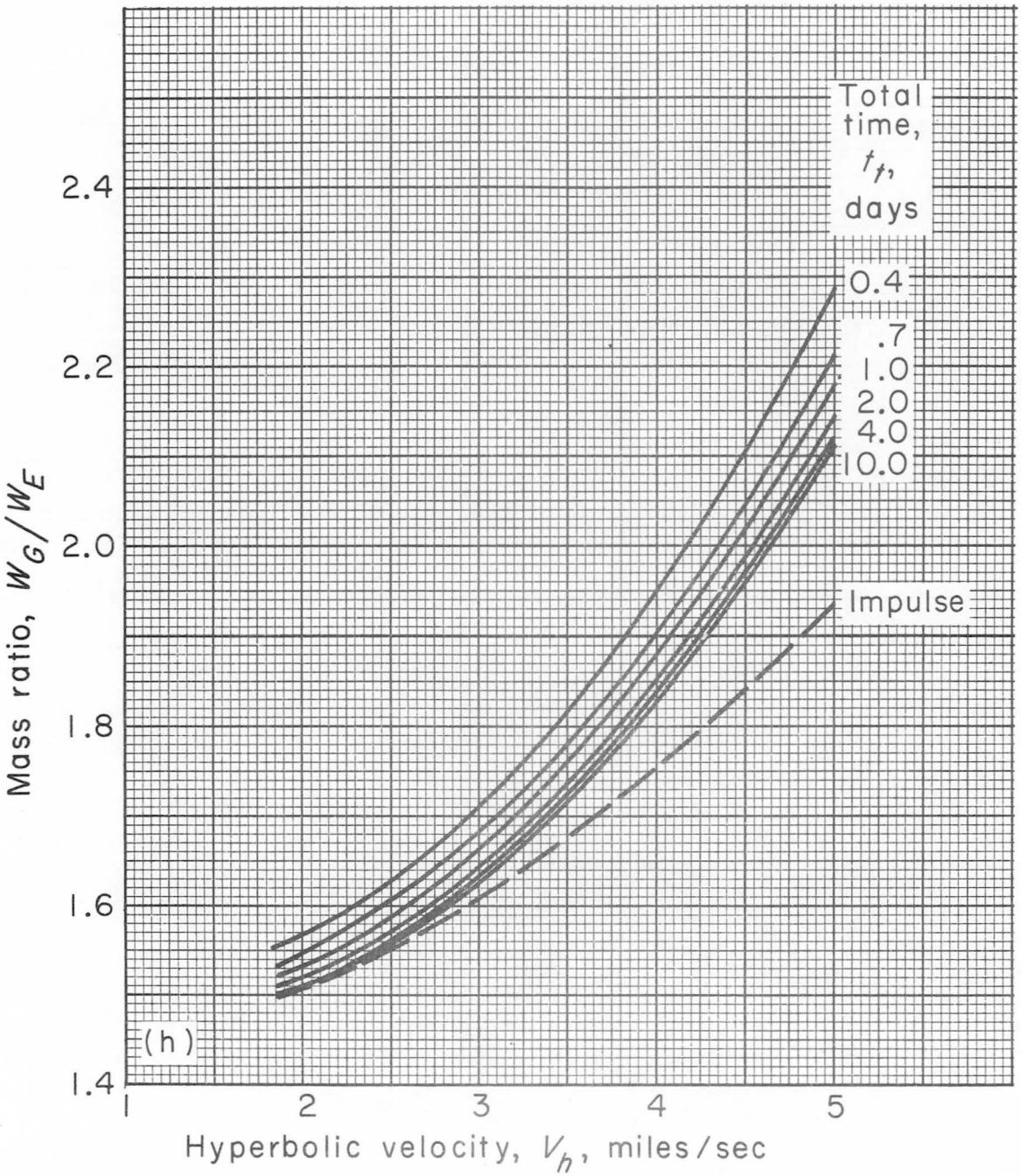

(h) Thrust-weight ratio, 0.05; specific impulse, 900 pounds per pound per second.

Figure 8. - Continued. Variation of mass ratio with hyperbolic velocity. β, 0°; optimum $\Delta\theta_1$ and $\Delta\theta_2$.

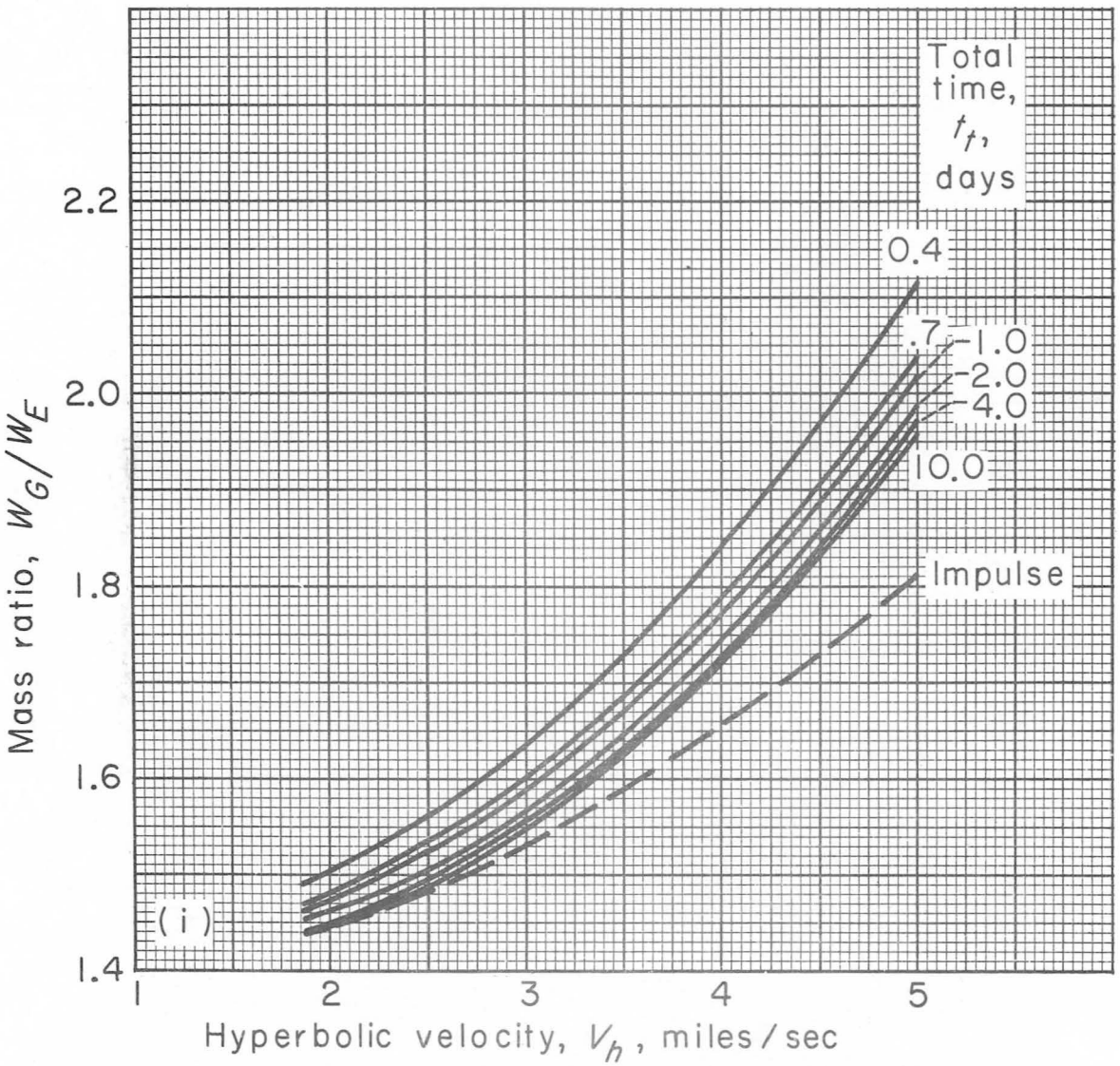

(i) Thrust-weight ratio, 0.05; specific impulse, 1000 pounds per pound per second.

Figure 8. - Concluded. Variation of mass ratio with hyperbolic velocity. β, 0°; optimum $\Delta\theta_1$ and $\Delta\theta_2$.

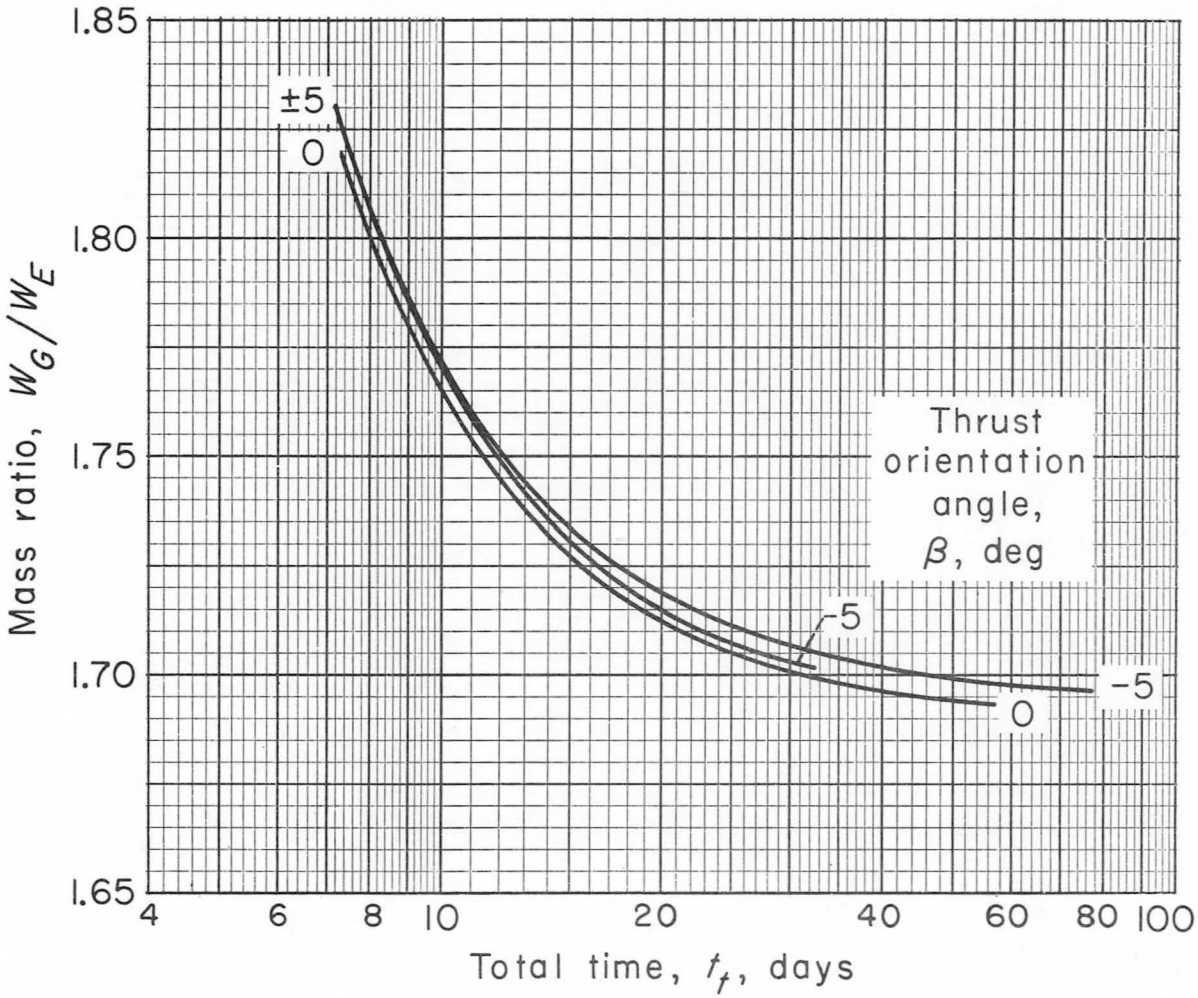

Figure 9. - Optimization of thrust angle. Specific impulse, 1000 pounds per pound per second, thrust-weight ratio 0.01; hyperbolic velocity, 3.0 miles per second; $\Delta\theta_1$, 0°; $\Delta\theta_2$, 50°.

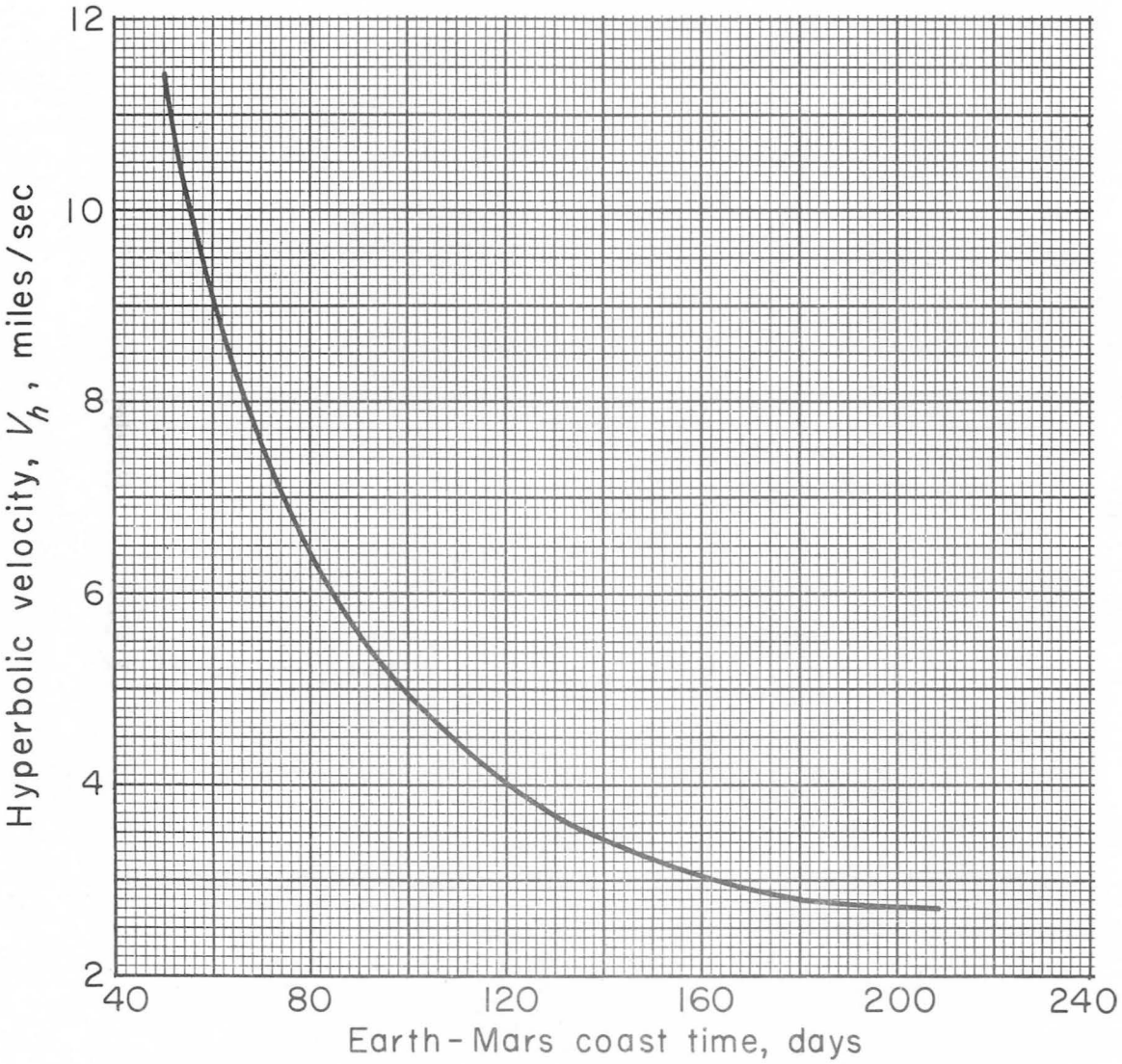

Figure 10. - Minimum hyperbolic velocities for 1960 Mars probes from three-dimensional actual-orbit analysis.

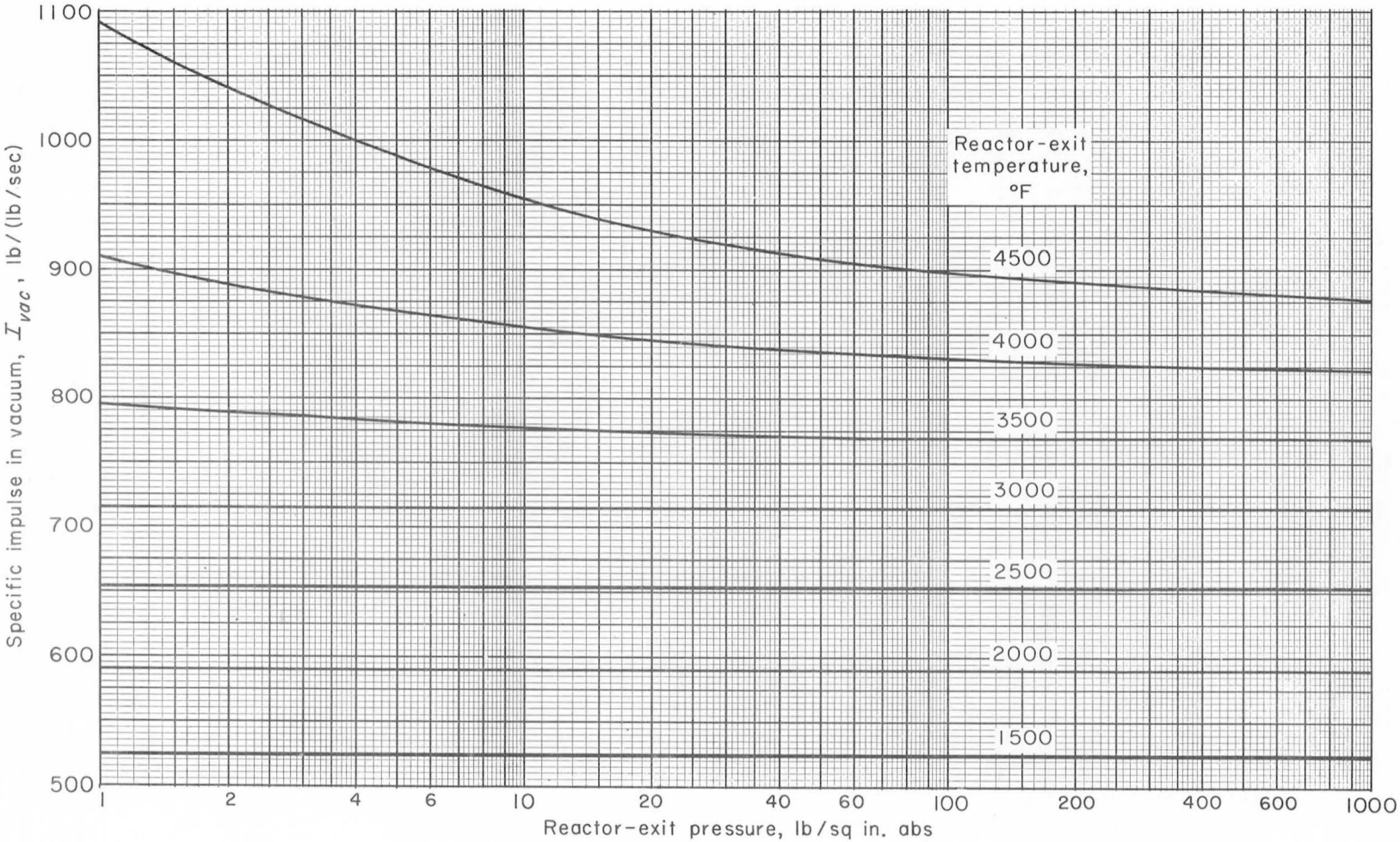

Figure 11. - Variation of specific impulse in vacuum with reactor-exit hydrogen pressure and temperature. Equilibrium expansion; nozzle velocity correction factor, 0.96; nozzle expansion ratio, 50.

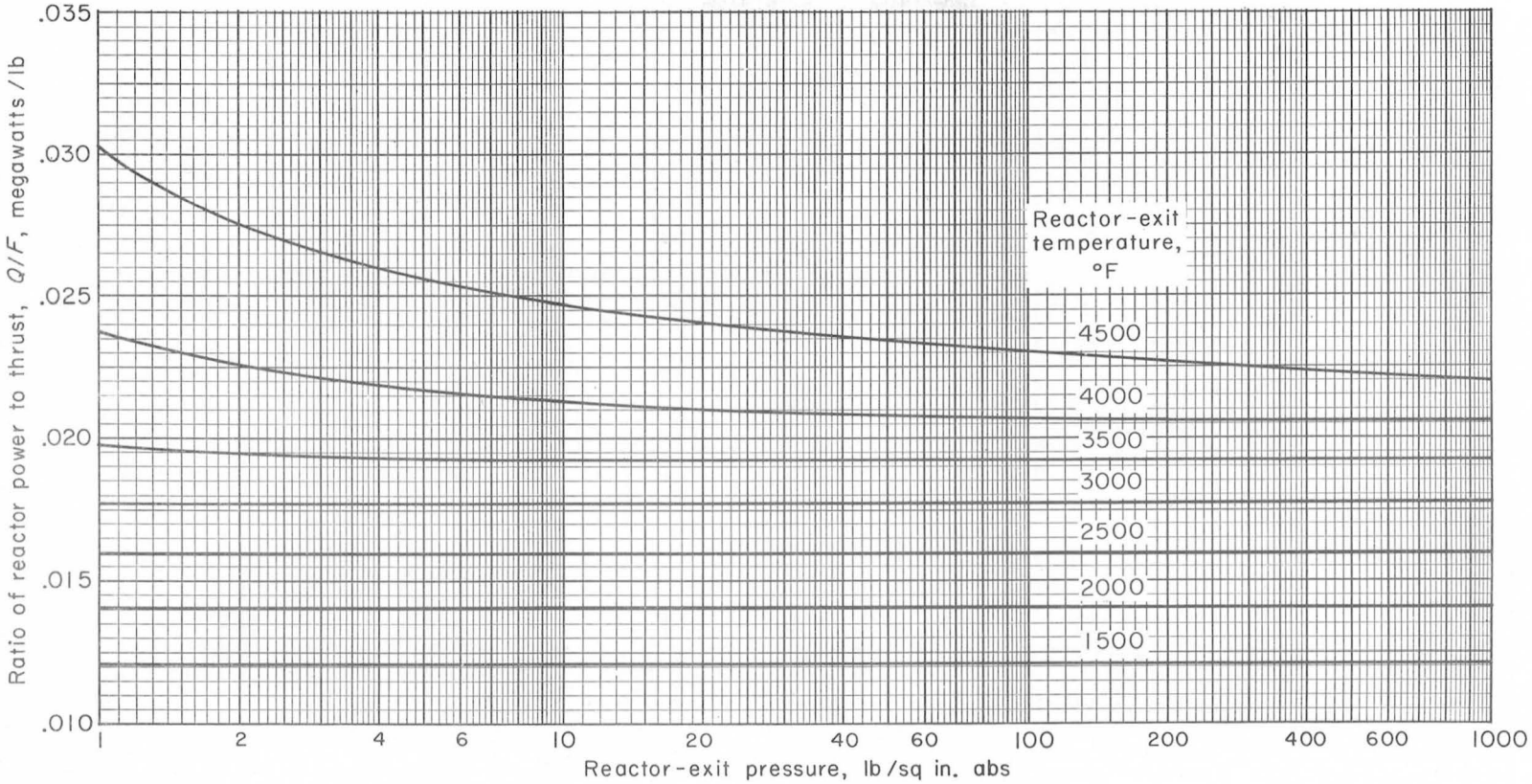

Figure 12. - Variation of reactor-power-to-thrust ratio with reactor-exit hydrogen pressure and temperature. Equilibrium expansion; nozzle velocity correction factor, 0.96; reactor-inlet temperature, 200° R; nozzle expansion ratio, 50.

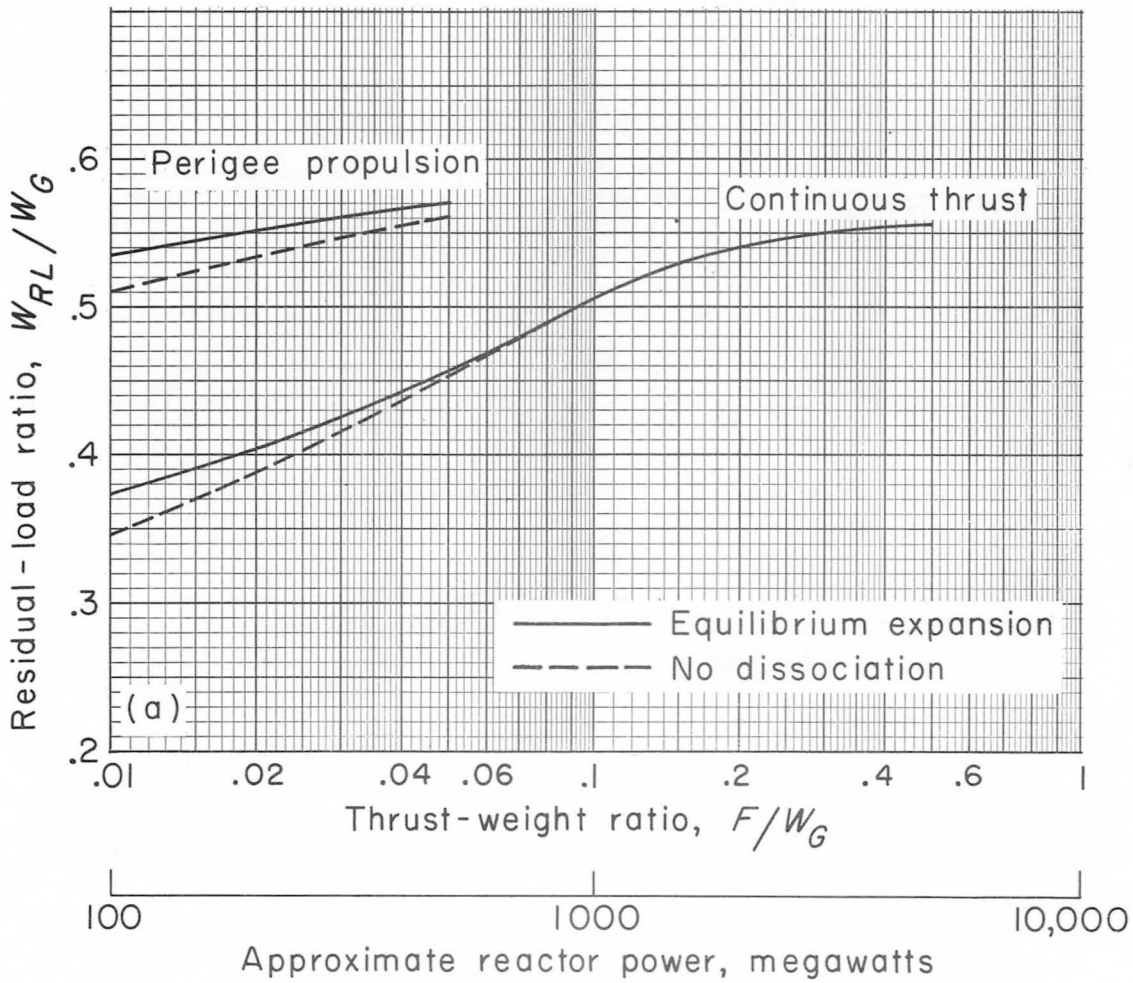

(a) Gross weight, 500,000 pounds.

Figure 13. - Performance comparison of perigee propulsion and continuous thrust. Mission time, 209 days; reactor exit temperature, 4500° F.

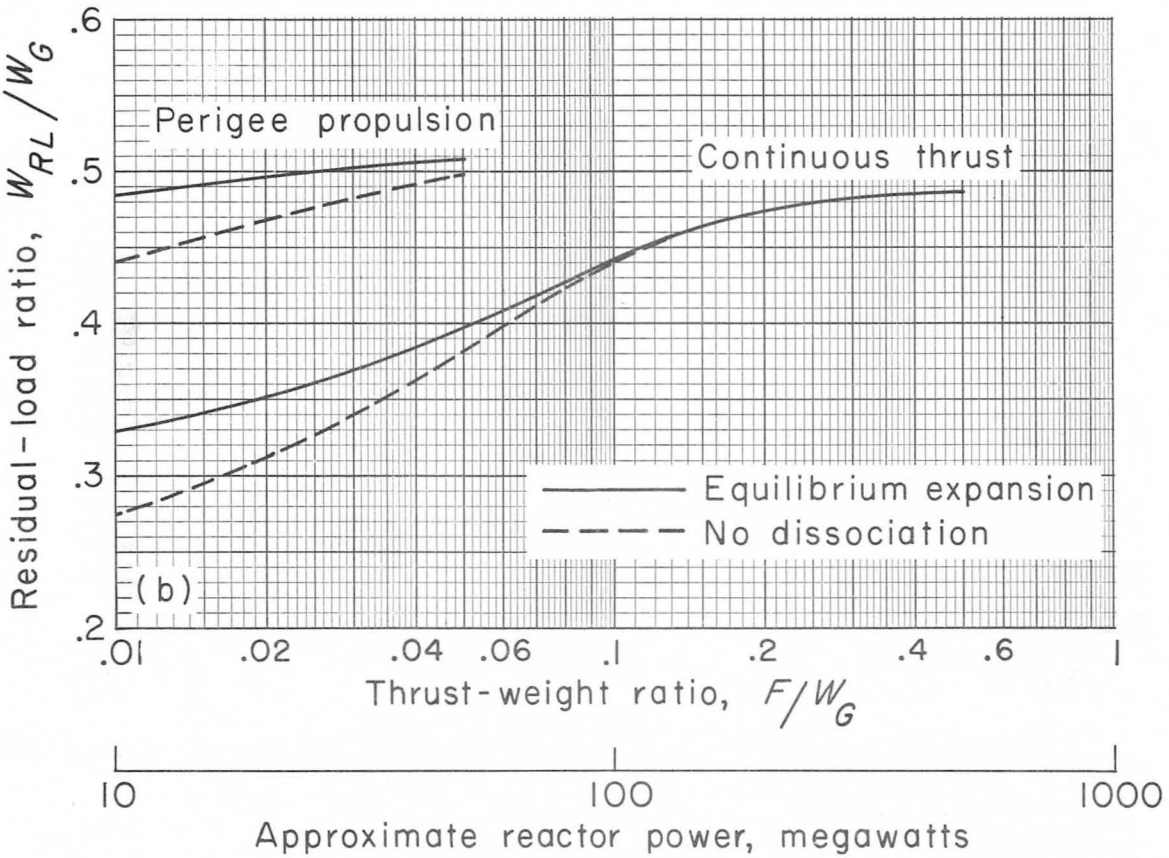

(b) Gross weight, 50,000 pounds.

Figure 13. - Concluded. Performance comparison of perigee propulsion and continuous thrust. Mission time, 209 days; reactor exit temperature, 4500° F.